



# Improving polygenic prediction in ancestrally diverse populations

Yunfeng Ruan<sup>1,2</sup>, Yen-Feng Lin<sup>3,4,5</sup>, Yen-Chen Anne Feng<sup>1,6,7,8,9,10</sup>, Chia-Yen Chen<sup>11</sup>, Max Lam<sup>1,8,12,13,14</sup>, Zhenglin Guo<sup>1</sup>, Stanley Global Asia Initiatives\*, Lin He<sup>2</sup>, Akira Sawa<sup>15</sup>, Alicia R. Martin<sup>1,8,16</sup>, Shengying Qin<sup>1,2,60</sup>✉, Hailiang Huang<sup>1,8,16,60</sup>✉ and Tian Ge<sup>1,6,7,17,60</sup>✉

**Polygenic risk scores (PRS) have attenuated cross-population predictive performance. As existing genome-wide association studies (GWAS) have been conducted predominantly in individuals of European descent, the limited transferability of PRS reduces their clinical value in non-European populations, and may exacerbate healthcare disparities. Recent efforts to level ancestry imbalance in genomic research have expanded the scale of non-European GWAS, although most remain underpowered. Here, we present a new PRS construction method, PRS-CSx, which improves cross-population polygenic prediction by integrating GWAS summary statistics from multiple populations. PRS-CSx couples genetic effects across populations via a shared continuous shrinkage (CS) prior, enabling more accurate effect size estimation by sharing information between summary statistics and leveraging linkage disequilibrium diversity across discovery samples, while inheriting computational efficiency and robustness from PRS-CS. We show that PRS-CSx outperforms alternative methods across traits with a wide range of genetic architectures, cross-population genetic overlaps and discovery GWAS sample sizes in simulations, and improves the prediction of quantitative traits and schizophrenia risk in non-European populations.**

Human complex traits and diseases are influenced by hundreds or thousands of genetic variants, each explaining a small proportion of phenotypic variation. PRS aggregate genetic effects across the genome to measure the overall genetic liability to a trait or disease. PRS are not useful as a stand-alone diagnostic tool; rather, they have shown promise in predicting individualized disease risk and trajectories, stratifying patient groups, informing preventive, diagnostic and therapeutic strategies, and improving biomedical and health outcomes<sup>1–6</sup>.

Despite the potential for clinical translation, recent theoretical and empirical studies showed that PRS have decreased cross-population prediction accuracy, especially when the discovery and target samples are genetically distant<sup>7–10</sup>. As existing GWAS have been conducted predominantly in individuals of European descent<sup>11–14</sup>, the poor transferability of PRS across populations has impeded its clinical implementation and raised health disparity concerns<sup>7</sup>. Therefore, there is an urgent need to improve the accuracy of cross-population polygenic prediction to maximize the clinical potential of PRS and ensure equitable delivery of precision medicine to global populations.

As efforts to diversify samples in genomic research start to grow, the scale of non-European genomic resources has been expanded

in recent years. Although the sample sizes of most non-European GWAS remain considerably smaller than European studies, they provide critical information on the variation of genetic effects across populations. Initial studies have indicated that the genetic architectures of many complex traits and diseases are largely concordant between populations—both at the single-variant level and at the genome-wide level<sup>15–18</sup>, suggesting that the transferability of PRS may be improved by integrating GWAS summary statistics from diverse populations. However, current PRS construction methods have been designed primarily for applications in one homogeneous population<sup>19–23</sup>. Existing methods that can take GWAS summary statistics from multiple populations use meta-analysis to summarize genetic effects across training datasets<sup>24,25</sup>, but this approach does not model population-specific allele frequencies and linkage disequilibrium (LD) patterns. Alternatively, independent analysis can be performed on each discovery GWAS and the resulting PRS can be combined linearly<sup>26,27</sup>, but this approach does not make full use of the genetic overlap between populations to inform PRS construction.

Here, we present PRS-CSx, an extension of PRS-CS<sup>19</sup>, that improves cross-population polygenic prediction by jointly modeling GWAS summary statistics from multiple populations.

<sup>1</sup>Stanley Center for Psychiatric Research, Broad Institute of MIT and Harvard, Cambridge, MA, USA. <sup>2</sup>Bio-X Institutes, Key Laboratory for the Genetics of Developmental and Neuropsychiatric Disorders (Ministry of Education), Shanghai Jiao Tong University, Shanghai, China. <sup>3</sup>Center for Neuropsychiatric Research, National Health Research Institutes, Miaoli, Taiwan. <sup>4</sup>Department of Public Health and Medical Humanities, School of Medicine, National Yang Ming Chiao Tung University, Taipei, Taiwan. <sup>5</sup>Institute of Behavioral Medicine, College of Medicine, National Cheng Kung University, Tainan, Taiwan. <sup>6</sup>Department of Psychiatry, Massachusetts General Hospital, Harvard Medical School, Boston, MA, USA. <sup>7</sup>Psychiatric and Neurodevelopmental Genetics Unit, Center for Genomic Medicine, Massachusetts General Hospital, Boston, MA, USA. <sup>8</sup>Analytic and Translational Genetics Unit, Massachusetts General Hospital, Boston, MA, USA. <sup>9</sup>Institute of Epidemiology and Preventive Medicine, National Taiwan University, Taipei, Taiwan. <sup>10</sup>Master of Public Health Program, National Taiwan University, Taipei, Taiwan. <sup>11</sup>Biogen, Cambridge, MA, USA. <sup>12</sup>Division of Psychiatry Research, The Zucker Hillside Hospital, Northwell Health, Glen Oaks, NY, USA. <sup>13</sup>Research Division, Institute of Mental Health Singapore, Singapore, Singapore. <sup>14</sup>Human Genetics, Genome Institute of Singapore, Singapore, Singapore. <sup>15</sup>Departments of Psychiatry, Neuroscience, Biomedical Engineering, Genetic Medicine, and Mental Health, Johns Hopkins University School of Medicine and Bloomberg School of Public Health, Baltimore, MD, USA. <sup>16</sup>Department of Medicine, Harvard Medical School, Boston, MA, USA. <sup>17</sup>Center for Precision Psychiatry, Massachusetts General Hospital, Boston, MA, USA. <sup>60</sup>These authors jointly supervised this work: Shengying Qin, Hailiang Huang, Tian Ge. \*A list of authors and their affiliations appears at the end of the paper. ✉e-mail: chinsir@sjtu.edu.cn; hhuang@broadinstitute.org; tge1@mgh.harvard.edu

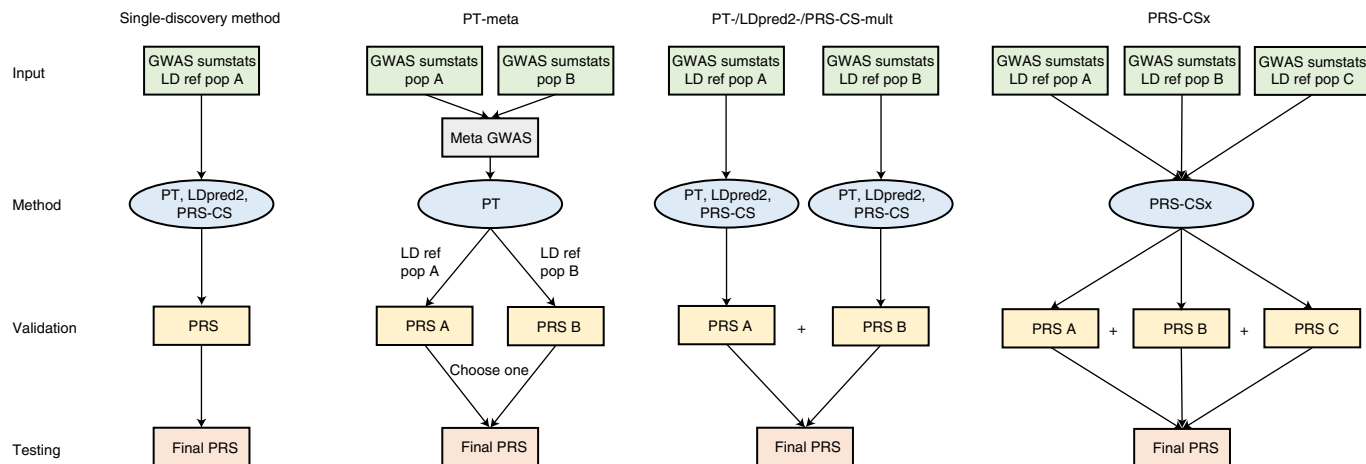


**Fig. 1 | Overview of polygenic prediction methods.** The predictive performances of three representative single-discovery (PT, LDpred2 and PRS-CS) and five multi-discovery (PT-meta, PT-mult, LDpred2-mult, PRS-CS-mult and PRS-CSx) methods are compared in this study. LDpred2-mult and PRS-CS-mult depicted here are not published methods but are helpful for comparing potential improvements from PRS-CSx, which uses a coupled CS prior for the effect sizes of genetic variants. The discovery samples (to generate GWAS summary statistics (sumstats)), validation samples (to tune hyperparameters in PRS construction methods) and testing samples (to assess prediction accuracy) are nonoverlapping. LD ref, LD reference panel; pop A/B/C, Population A/B/C.

We compare the predictive performance of PRS-CSx with existing PRS construction methods across traits with a wide range of genetic architectures, cross-population genetic overlaps and discovery GWAS sample sizes via simulations. We further apply PRS-CSx to predict quantitative traits using data from the UK Biobank (UKBB)<sup>28</sup>, Biobank Japan (BBJ)<sup>29,30</sup>, the Population Architecture using Genomics and Epidemiology Consortium (PAGE) study<sup>31</sup> and the Taiwan Biobank (TWB)<sup>32,33</sup>, and predict schizophrenia risk using cohorts of European and East Asian ancestries<sup>15,34</sup>.

## Results

**Overview of PRS-CSx.** PRS-CSx extends PRS-CS<sup>19</sup>—a recently developed Bayesian polygenic modeling and prediction framework—to improve cross-population polygenic prediction by integrating GWAS summary statistics from multiple ancestry groups (Methods). PRS-CSx uses a shared continuous shrinkage prior to couple SNP effects across populations, which enables more accurate effect size estimation by sharing information between summary statistics and leveraging LD diversity across discovery samples. The shared prior allows for correlated but varying effect size estimates across populations, retaining the flexibility of the modeling framework. In addition, PRS-CSx explicitly models population-specific allele frequencies and LD patterns, and inherits from PRS-CS the computational advantages of CS priors, and the efficient and robust posterior inference algorithm (Gibbs sampling). Given GWAS summary statistics and ancestry-matched LD reference panels, PRS-CSx calculates one polygenic score for each discovery sample, and integrates them by learning an optimal linear combination to produce the final PRS (Fig. 1).

**Overview of PRS analysis.** We have broadly classified polygenic prediction methods into two categories: single-discovery methods, which train PRS using GWAS summary statistics from a single-discovery sample; and multi-discovery methods, which combine GWAS summary statistics from multiple discovery samples for PRS construction. In this work, in addition to PRS-CSx, we assess and compare within- and cross-population predictive performance of three representative single-discovery (LD-informed pruning and *P* value thresholding (PT)<sup>35</sup>, LDpred2 (ref. 20) and PRS-CS<sup>19</sup>) and four multi-discovery (PT-meta, PT-mult<sup>26</sup>, LDpred2-mult and PRS-CS-mult) methods. PT-meta applies PT to the meta-analyzed

discovery GWAS summary statistics. The three ‘mult’ methods respectively apply PT, LDpred2 and PRS-CS to each discovery GWAS separately, and linearly combine the resulting PRS. PT-mult has been demonstrated to improve the prediction in recently admixed populations<sup>26</sup>. Here, we have extended the idea of PT-mult to LDpred2-mult and PRS-CS-mult, creating two new methods to quantify the benefits of jointly modeling multiple GWAS summary statistics via the coupled shrinkage prior. The workflow for each PRS construction method is shown in Fig. 1. In all the PRS analyses, we use the discovery dataset to estimate the marginal effect sizes of genetic variants and generate GWAS summary statistics for each population; we use the validation dataset, with individual-level genotypes and phenotypes, to tune hyperparameters for different polygenic prediction methods; and we use the testing dataset, with individual-level genotypes and phenotypes, to evaluate the prediction accuracy of PRS and compute performance metrics using hyperparameters learnt in the validation dataset. The three datasets comprise nonoverlapping individuals. For convenience, we use the target dataset to refer to the combination of validation and testing datasets, which have matched ancestry. For fair comparison, throughout the paper we use 1000 Genomes Project (1KG) Phase 3 (ref. 36) superpopulation samples (European (EUR)  $N=503$ ; East Asian (EAS)  $N=504$ ; African (AFR)  $N=661$ ; admixed American (AMR)  $N=347$ ) as the LD reference panels across different PRS construction methods.

**Simulations.** We first evaluated the predictive performance of different polygenic prediction methods via simulations. We simulated individual-level genotypes of EUR, EAS and AFR populations for HapMap3 variants with minor allele frequency (MAF)  $>1\%$  in at least one of the three populations using HAPGEN2 (ref. 37), with the 1KG Phase 3 samples as the reference panel. In our primary simulation setting, we randomly sampled 1% HapMap3 variants as causal variants, which, in aggregation, explained 50% of phenotypic variation in each population. We assumed that causal variants are shared across populations but allowed for varying effect sizes, which were sampled from a multivariate normal distribution with the cross-population genetic correlation ( $r_g$ ) set to 0.7. The simulation was repeated 20 times.

We first applied single-discovery methods to GWAS summary statistics generated by 100,000 simulated EUR samples and 20,000

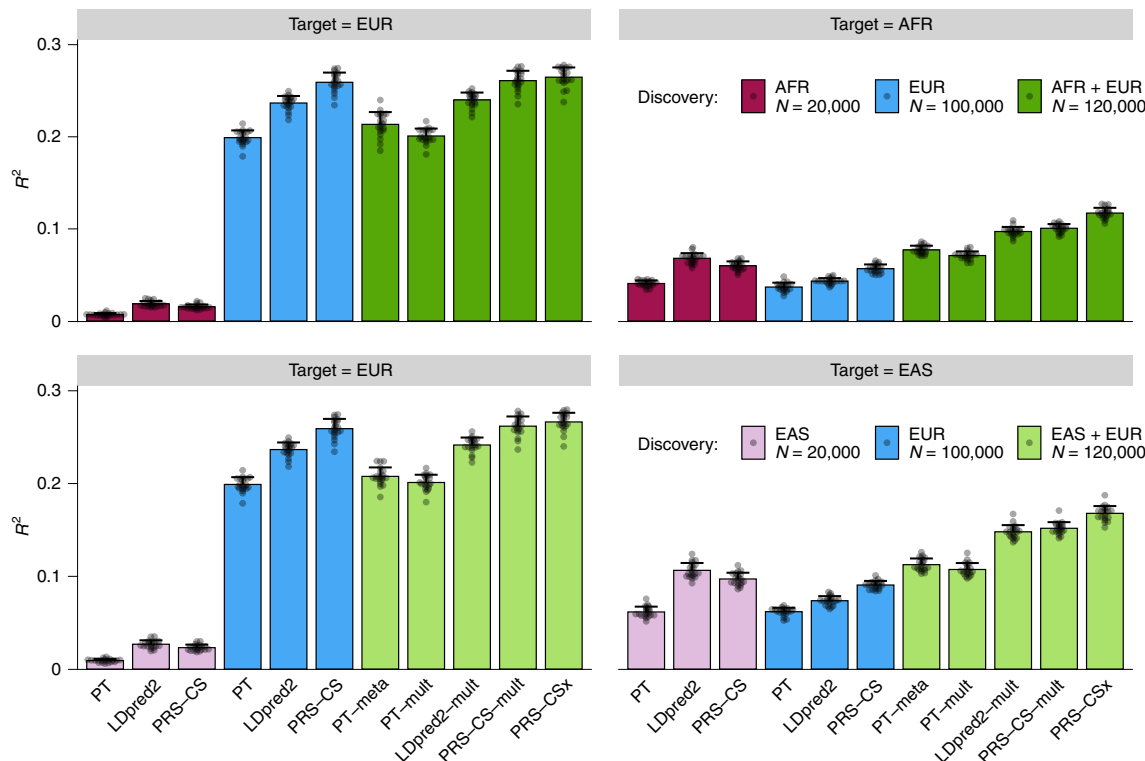


**Fig. 2 | Prediction accuracy of single-discovery and multi-discovery polygenic prediction methods in simulations.** 1% HapMap3 variants were randomly sampled as causal variants, which, in aggregation, explained 50% of phenotypic variation in each population. Causal variants were shared across populations with a cross-population genetic correlation of 0.7; 100,000 simulated EUR samples and 20,000 non-EUR (EAS or AFR) samples were used as the discovery dataset. Each bar shows the squared correlation ( $R^2$ ) between the simulated and predicted phenotypes for a polygenic prediction method in an independent testing dataset, averaged across 20 simulation replicates. Error bar indicates s.d. of  $R^2$  across replicates. Prediction accuracy for each simulation replicate is overlaid on the bar plot.

non-EUR (EAS or AFR) samples, and evaluated their predictive performance, measured by the squared correlation ( $R^2$ ) between the simulated and predicted phenotypes, in 20,000 target samples, which were evenly split into a validation dataset and a testing dataset (Fig. 2 and Supplementary Table 1). As expected, when the target population was EUR, PRS trained on the larger EUR GWAS were substantially more accurate than PRS trained on non-EUR GWAS (Fig. 2; left panels). However, when the target population was EAS or AFR, PRS trained on ancestry-matched non-EUR GWAS were more predictive than EUR PRS (Fig. 2; right panels), even though the sample sizes of the non-EUR GWAS were much smaller (20,000 versus 100,000). Among the three single-discovery methods examined, Bayesian methods (LDpred2 and PRS-CS) consistently outperformed PT. PRS-CS seemed to be more accurate than LDpred2 in both within- and cross-population prediction when the discovery GWAS was well-powered, while LDpred2 was more accurate when the discovery sample size was limited, probably reflecting the strengths and limitations of the different priors used in PRS-CS and LDpred2 (Supplementary Note).

We then assessed whether multi-discovery methods can improve cross-population polygenic prediction. Specifically, we used different multi-discovery methods to combine GWAS summary statistics from 100,000 EUR samples and 20,000 non-EUR (EAS or AFR) samples as the discovery dataset, and evaluated their predictive performance in independent target samples (Fig. 2 and Supplementary Table 1). Figure 2 shows that, in general, multi-discovery methods improved prediction accuracy over their single-discovery counterparts (that is, PT-meta or PT-mult versus PT; LDpred2-mult versus LDpred2; PRS-CS-mult versus PRS-CS), reflecting the increase in discovery sample size. When the target population was EUR,

the improvement of PRS-CSx and PRS-CS-mult over PRS-CS was marginal, suggesting that the benefits of adding a small non-EUR GWAS to the discovery dataset can be limited in this case. However, when predicting into non-EUR populations, multi-discovery methods clearly outperformed single-discovery methods, with Bayesian methods (LDpred2-mult, PRS-CS-mult and PRS-CSx) demonstrating a larger advantage over PT-based methods. PRS-CSx provided an additional increase of 10.6% and 16.4% in  $R^2$  over PRS-CS-mult when the target populations were EAS and AFR, respectively, demonstrating that joint modeling of the genetic architecture across populations using the coupled continuous shrinkage prior improves polygenic prediction in non-EUR populations.

We conducted a series of secondary simulations, by varying one parameter in the primary simulation at a time, to assess the generalizability of the above observations and the robustness of PRS-CSx across a wide range of genetic architectures, cross-population genetic overlaps and discovery GWAS sample sizes (Extended Data Figs. 1–7 and Supplementary Tables 2–9; Supplementary Note). We concluded that, while the benefits of using a coupled prior varied with simulation designs and may be small in certain scenarios, PRS-CSx improved cross-population prediction accuracy relative to alternative methods across most simulation settings and was robust to model misspecification.

**Prediction of quantitative traits in Biobanks.** Next, we evaluated the predictive performance of different polygenic prediction methods using 33 anthropometric or blood panel traits from UKBB<sup>28</sup> ( $N=314,916$ – $360,388$ ) and BBJ<sup>30</sup> ( $N=71,221$ – $165,419$ ; Supplementary Table 10). All 33 traits, with two exceptions (Basophil and Eosinophil), had moderate-to-high cross-population

genetic-effect correlations estimated by POPCORN<sup>16</sup> (range 0.37–0.85; Supplementary Table 10). We applied single-discovery methods to UKBB or BBJ summary statistics, and used multi-discovery methods to combine UKBB and BBJ GWAS. All target samples are unrelated UKBB individuals that are also unrelated with the UKBB discovery samples. We assigned each target sample to one of the five 1KG superpopulations [AFR, AMR, EAS, EUR, SAS (South Asian)] (Methods), and assessed the prediction accuracy in each target population separately, adjusting for age, sex and top 20 principal components (PCs) of the genotypes. For each population, the target dataset was split randomly and evenly into a validation dataset and a testing dataset. The prediction accuracy, measured by variance explained ( $R^2$ ) in linear regression after adjusting for covariates, was averaged across 100 random splits.

Consistent with simulation results, Bayesian multi-discovery methods examined here (LDpred2-mult, PRS-CS-mult and PRS-CSx) often outperformed published single-discovery methods and PT-based multi-discovery methods, suggesting the importance of integrating available GWAS summary statistics and appropriately accounting for population-specific LD patterns in cross-population prediction (Fig. 3 and Supplementary Table 11). The improvement of PRS-CSx in prediction accuracy relative to LDpred2 and PRS-CS trained on UKBB summary statistics (which were, on average, more accurate than PRS trained on BBJ GWAS), and LDpred2-mult and PRS-CS-mult (which were often the second and third best multi-discovery method) depended on the target population.

When predicting into the EUR population, PRS-CSx provided a consistent but marginal improvement over LDpred2 (median relative increase in  $R^2$ : 4.7%) and PRS-CS (median relative increase in  $R^2$ : 5.2%), probably due to the limited power of the BBJ GWAS relative to the UKBB GWAS in EUR prediction. The benefit of the coupled prior in this case was also limited, as reflected by a small improvement of PRS-CSx relative to PRS-CS-mult (median relative increase in  $R^2$ : 2.2%; Fig. 3a, left panel and Supplementary Table 11), which was consistent with the observations in simulations. When the target population was EAS, however, PRS-CSx substantially increased the prediction accuracy relative to single-discovery methods: the median relative improvements in  $R^2$  were 52.3% and 32.9%, respectively, when compared with LDpred2 and PRS-CS trained on UKBB GWAS, and 69.8% and 74.4%, respectively, when compared with LDpred2 and PRS-CS trained on BBJ GWAS, suggesting that PRS-CSx can leverage large-scale EUR GWAS to improve the prediction in non-EUR populations. PRS-CSx also had a median improvement of 10.5% (two-sided Wilcoxon signed-rank test  $P_{\text{wilcoxon}} = 3.90 \times 10^{-4}$ ) and 8.3% ( $P_{\text{wilcoxon}} = 2.84 \times 10^{-6}$ ) relative to LDpred2-mult and PRS-CS-mult, respectively, demonstrating the benefits of jointly modeling summary statistics from multiple populations in trans-ancestry prediction (Fig. 3a, middle panel and Supplementary Table 11). When the target population did not match any of the discovery samples, PRS-CSx was still able to increase the prediction accuracy. For example, when predicting into the AFR population, the median improvements of PRS-CSx relative to LDpred2 and PRS-CS trained on UKBB GWAS were 45.1% and 16.9%, respectively, and the median improvements relative to LDpred2-mult and PRS-CS-mult were 22.2% ( $P_{\text{wilcoxon}} = 2.38 \times 10^{-5}$ ) and 7.1% ( $P_{\text{wilcoxon}} = 2.99 \times 10^{-5}$ ), respectively (Fig. 3a, right panel and Supplementary Table 11).

We next sought to replicate the relative performance of different PRS construction methods in the Taiwan Biobank (TWB)<sup>32</sup>, which is a community-based prospective cohort study of the Taiwanese population. Among the 33 quantitative traits we examined in UKBB and BBJ, 21 were also available in TWB. All PRS were trained on the UKBB and/or BBJ GWAS, validated in the UKBB EAS samples (where hyperparameters were learnt; Supplementary Table 12), and evaluated in the TWB sample comprising 10,149 unrelated individuals, adjusting for age, sex and top 20 PCs of the genotypes. Figure 3b

shows that single-discovery methods trained on UKBB and BBJ GWAS had similar performance in the TWB sample, even though UKBB GWAS were much larger (Fig. 3b and Supplementary Table 13). Bayesian multi-discovery methods showed substantial improvement in prediction accuracy compared with single-discovery methods. PRS-CSx provided a median improvement of 39.5% relative to PRS-CS (the best single-discovery method) and 8.2% relative to PRS-CS-mult (the second best multi-discovery method), suggesting the robustness of PRS-CSx when model parameters learnt in validation datasets were applied to external independent testing datasets. Overall, results in the TWB closely reproduced the patterns observed in the UKBB EAS samples (Fig. 3a, middle panel).

We further investigated whether adding African American samples to the discovery dataset can improve the prediction in the AFR population. Among the 33 traits we examined, 14 were also available in PAGE<sup>31</sup> ( $N=11,178$ –49,796), a genetic epidemiology study comprising largely African American and Hispanic/Latino samples (Supplementary Table 10). All UKBB-PAGE and BBJ-PAGE genetic-effect correlations were moderate-to-high (range 0.44–1.00; Supplementary Table 10). Although the discovery and target samples had largely matched ancestry, applying PRS-CS (or other single-discovery methods) to PAGE summary statistics alone produced low prediction accuracy in the AFR population with only a few exceptions, due to the small sample size of the PAGE study (Fig. 3c and Supplementary Table 14). However, integrating UKBB, BBJ and PAGE summary statistics using PRS-CSx (Supplementary Table 15) dramatically outperformed single-discovery methods, and the median relative improvement in  $R^2$  was 28.1% when compared with PRS-CSx trained on UKBB and BBJ GWAS only, suggesting that PRS-CSx benefits from including samples that have matched ancestry with the target population in the discovery dataset, even if the non-European GWAS included are considerably smaller than European studies (Fig. 3c and Supplementary Table 14). We note, however, that the overall prediction accuracy in the AFR population remained low relative to the predictions in EUR and EAS individuals, reflecting highly imbalanced sample sizes in the training GWAS across populations (Extended Data Fig. 8). We additionally assessed the convergence of the model fitting algorithm used in PRS-CSx, and confirmed that the Gibbs sampler achieved reasonable convergence and mixing<sup>38</sup> (Extended Data Fig. 9; Supplementary Note).

**Schizophrenia risk prediction.** Last, we evaluated the predictive performance of different polygenic prediction methods for dichotomous traits. We used schizophrenia as an example, for which large-scale EUR and EAS GWAS along with multiple individual-level cohorts are available (Supplementary Table 16). Specifically, we used GWAS summary statistics derived from the Psychiatric Genomics Consortium (PGC) wave 2 EUR samples (33,640 cases and 43,456 controls)<sup>34</sup> and ten PGC EAS cohorts<sup>15</sup> (7,856 cases and 11,562 controls) as the discovery dataset. For the additional seven EAS cohorts for which we had access to individual-level data, we set aside one cohort (KOR1; 687 cases and 492 controls) as the validation dataset (for hyperparameter tuning), and applied a leave-one-out approach to the remaining six cohorts. More specifically, we used one of the six cohorts in turn as the testing dataset, and meta-analyzed the remaining five cohorts with the ten PGC EAS cohorts using an inverse-variance-weighted meta-analysis to generate the discovery GWAS summary statistics for the EAS population. The prediction accuracy of different PRS construction methods was then evaluated in the left-out (testing) cohort, adjusting for sex and top 20 PCs.

Consistent with previous observations, PRS trained on EAS GWAS were more predictive in EAS cohorts than those trained on PGC EUR summary statistics<sup>15</sup>, despite the larger sample size for the EUR GWAS (Fig. 4a and Supplementary Table 17). Among single-discovery methods examined, LDpred2 and PRS-CS

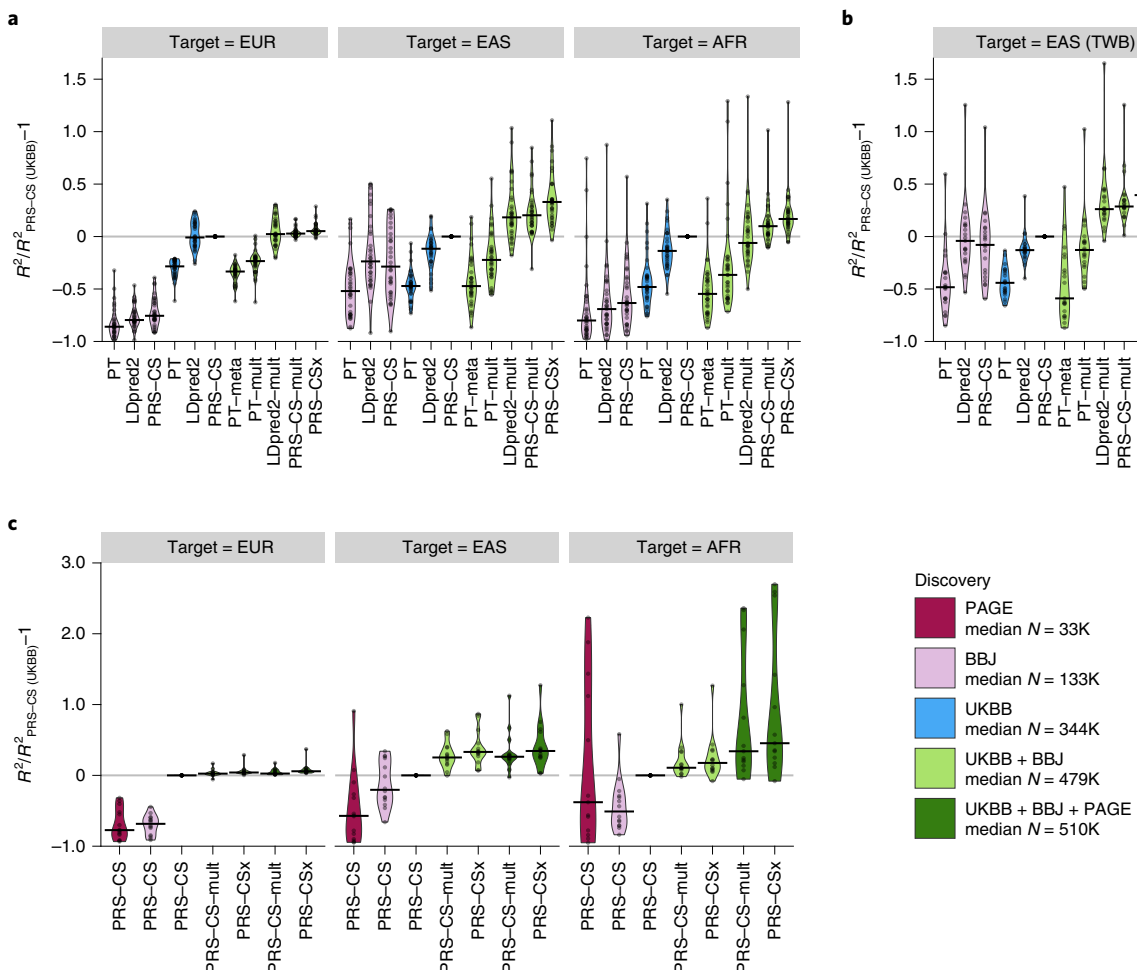


**Fig. 3 | Relative prediction accuracy for quantitative traits in each target population.** **a–c**, Relative prediction performance for single-discovery and multi-discovery PRS construction methods using discovery GWAS summary statistics from UKBB and BBJ, across 33 traits, in different UKBB target populations (EUR, EAS and AFR) (**a**); from UKBB and BBJ, across 21 traits, in the Taiwan Biobank (TWB) (**b**); from UKBB, BBJ and PAGE, across 14 traits, in different UKBB target populations (EUR, EAS and AFR) (**c**). Each datapoint shows the relative increase of prediction performance, defined as  $R^2/R^2_{\text{PRS-CS (UKBB)}} - 1$ , in which  $R^2_{\text{PRS-CS (UKBB)}}$  is the  $R^2$  of the trait in the same target population using PRS-CS trained on the UKBB GWAS summary statistics. In UKBB target populations (**a**, **c**),  $R^2$  was averaged across 100 random splits of the target samples into validation and testing datasets. The crossbar indicates the median of the relative increase of predictive performance across the traits examined. median N, median sample size across the respective discovery GWAS. The trait MCHC was not included in the AFR panel because its  $R^2$  from PRS-CS (UKBB) was almost 0, which inflated relative increase of prediction performance for other methods.

performed substantially better than PT, highlighting the importance of modeling LD patterns for highly polygenic traits. By integrating EUR and EAS summary statistics, Bayesian multi-discovery methods dramatically increased the prediction accuracy relative to single-discovery methods. Compared with LDpred2, the best-performing single-discovery method in this analysis, PRS-CSx increased the median  $R^2$  on the liability scale (assuming 1% of disease prevalence) from 0.043 (LDpred2 trained on EAS GWAS) and 0.031 (LDpred2 trained on EUR GWAS) to 0.063, a relative increase of 45.4% and 104.9%, respectively. PRS-CSx also approximately doubled the prediction accuracy of PT-meta and PT-mult, with a relative increase of 135.9% (from 0.027 to 0.063) and 95.3% (from 0.032 to 0.063) in the median liability  $R^2$ , respectively. In addition, PRS-CSx provided consistent, although relatively small, improvement over LDpred2-mult (relative increase in median  $R^2$ : 8.7%) and PRS-CS-mult (relative increase in median  $R^2$ : 5.9%), suggesting that, in practice, PRS-CSx can increase predictive power over Bayesian ‘mult’ methods even for highly polygenic architecture (Fig. 4a and Supplementary Table 17), a scenario where the benefit

of the coupled prior was reduced in simulations (Extended Data Fig. 1 and Supplementary Table 2). Other performance metrics, including Nagelkerke’s  $R^2$ , odds ratio (OR) per standard deviation change of PRS, and OR comparing top 10% with bottom 10% of the PRS distribution, showed a consistent pattern (Supplementary Table 17). Finally, PRS-CSx can more accurately identify individuals at high/low schizophrenia risk than alternative methods, showing a 2.9, 3.5 and 4.2-fold increase in the proportion of schizophrenia cases across the six testing cohorts when contrasting the top 10%, 5% or 2% of the PRS distribution with the bottom 10%, 5% or 2%, respectively (Fig. 4b and Supplementary Table 18).

## Discussion

We have presented PRS-CSx, a Bayesian polygenic prediction method that integrates GWAS summary statistics from multiple populations to improve the prediction accuracy of PRS in ancestrally diverse samples. PRS-CSx leverages the correlation of genetic effects and LD diversity across populations to more accurately localize association signals and increase the effective sample size of the

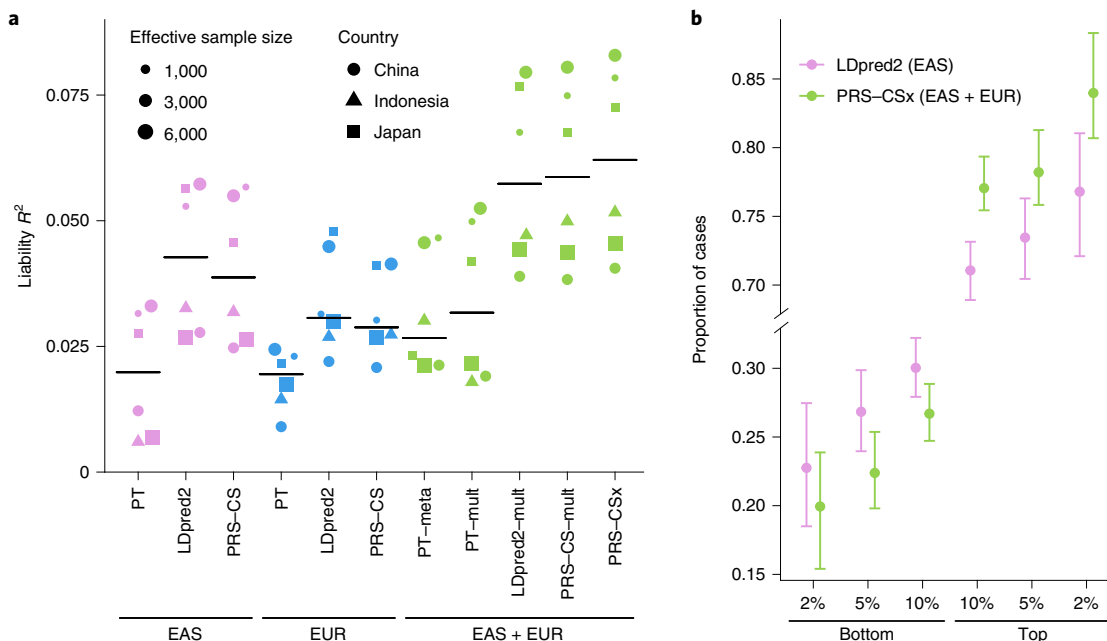


**Fig. 4 | Prediction accuracy of schizophrenia risk in EAS cohorts.** **a**, Prediction accuracy, measured as variance explained ( $R^2$ ) on the liability scale, of single-discovery (trained on EAS or EUR GWAS) and multi-discovery polygenic prediction methods (trained on both EAS and EUR GWAS: EAS + EUR) across six EAS schizophrenia cohorts. Each dot represents one testing cohort, with the size of the dot being proportional to its effective sample size, calculated as  $4/(1/N_{\text{case}}+1/N_{\text{control}})$ , and the shape of the dot representing the country where the sample was collected. Crossbar indicates the median  $R^2$  on the liability scale. **b**, The center of the error bar shows the proportion of schizophrenia cases of the bottom 2%, 5% and 10% and top 2%, 5% and 10% of the PRS distribution, constructed by LDpred2 trained on EAS GWAS (the best-performing single-discovery method) and PRS-CSx (the best-performing multi-discovery method), across six EAS schizophrenia cohorts (9,416 cases, 8,708 controls). Error bar, 95% confidence intervals.

discovery dataset, while accounting for population-specific allele frequency and LD patterns. We have shown, via simulation studies, that PRS-CSx robustly improves cross-population prediction over existing methods across traits with varying genetic architectures, genetic overlaps between populations and discovery GWAS sample sizes. Using quantitative traits from multiple biobanks as well as schizophrenia cohort studies of European and East Asian ancestries, we have further demonstrated that PRS-CSx can leverage large-scale European GWAS to boost the accuracy of polygenic prediction in non-European populations, for which ancestry-matched discovery GWAS may be orders of magnitude smaller in sample size.

PRS-CSx is expected to provide larger power gains when the GWAS in the target population has lower statistical power, while well-powered GWAS from other populations are available. This often happens when predicting into a non-EUR population, where ancestry-matched GWAS have limited sample sizes but large-scale EUR GWAS already exist. By integrating EUR and non-EUR GWAS, PRS-CSx can substantially improve the prediction accuracy in non-EUR populations, which alleviates the imminent challenge of polygenic prediction in under-represented populations. In contrast, PRS-CSx may provide limited increase in prediction accuracy when a well-powered GWAS in the target population already exists and GWAS from other populations have smaller sample sizes and lower statistical power. In practice, this happens almost exclusively for predictions in the EUR population. We note that, whereas PRS-CSx increased the prediction in non-European populations for most of the traits examined in this study, the amount of improvement in prediction accuracy over alternative methods varied across traits. Future research is needed to dissect the effects of potential factors on the accuracy of cross-ancestry polygenic prediction and to better understand the behavior of different prediction algorithms for individual traits.

PRS-CSx is designed to flexibly model GWAS summary statistics from multiple populations where SNP effect sizes and/or LD patterns differ. For two or more GWAS conducted in independent samples from the same population where effect sizes and LD patterns are expected to be highly concordant, a fixed-effect meta-analysis is probably the optimal approach to combine the GWAS and maximize statistical power. However, we do not recommend meta-analyzing summary statistics across populations and applying single-discovery methods (for example, LDpred2 or PRS-CS) to the meta-GWAS for two reasons: (1) the LD pattern of a cross-ancestry meta-analyzed GWAS is a mixture of population-specific LD, which is difficult to appropriately model. Rather, accurately modeling LD patterns is often crucial to the performance of Bayesian polygenic prediction methods. (2) The predictive performance of these ‘meta’ methods depends heavily on whether the assumption of the fixed-effect meta-analysis (that is, consistent SNP effects across populations) is accurate. These methods are thus less adaptive to a wide range of cross-population genetic architectures compared with PRS-CSx or the ‘mult’ methods. That said, many existing studies have released only summary statistics from cross-population meta-analysis, in which case applying single-discovery methods to the meta-GWAS remains a useful approach in practice. We believe that releasing ancestry-specific summary statistics from multi-ancestry genomic studies is critical for understanding comparative genetic architectures between populations, and for flexible and accurate cross-population polygenic modeling and prediction.

The use of PRS-CSx, as well as the ‘mult’ methods examined in this work, requires a validation dataset to tune hyperparameters and learn the optimal linear combination of population-specific PRS, and an independent testing dataset where the final PRS can be generated and evaluated. As non-European genomic resources remain limited, independent validation and testing datasets are often difficult

to identify, and a single target cohort may be too small to be split into validation and testing sets. To facilitate the use of PRS-CSx, we have released posterior SNP effects and linear combination weights for all the traits and target populations examined in this study. In addition, in certain applications, it may be preferable to calculate PRS for all samples in the target cohort rather than stratifying them into different ancestry groups. For example, returning genomic predictions to patients with recently admixed ancestries in clinical settings would be difficult as ancestries are not distinct entities, and genetic ancestry assignments may be inconsistent with self-reported race/ethnicity, illuminating the complexity of communicating population-stratified PRS results to patients. In these scenarios, PRS-CSx provides an ‘auto’ version which automatically learns the global shrinkage parameter from the discovery summary statistics, and a ‘meta’ option which integrates population-specific posterior SNP effects using an inverse-variance-weighted meta-analysis in the Gibbs sampler. Combining the ‘auto’ and ‘meta’ algorithms thus generates a trans-ancestry PRS that can be applied to all samples in the target cohort without the need for a validation dataset<sup>39</sup>. We note that, although simpler to implement, the ‘meta’ option is expected to be less accurate compared with the linear combination approach that optimizes PRS estimation separately in each target population.

Whereas PRS-CSx can take an arbitrary number of GWAS summary statistics as input, an ancestry-matched LD reference panel is required for each discovery sample, which may be challenging to build for GWAS conducted in admixed populations or in samples with large genomic diversity<sup>40</sup>. Although we have shown that PRS-CSx is robust to imperfectly matched LD reference panels, future work is needed to better model summary statistics from recently admixed populations<sup>41,42</sup>.

Finally, we note that, although PRS-CSx can improve cross-population polygenic prediction, the gap in the prediction accuracy between European and non-European populations remains considerable. Indeed, sophisticated statistical and computational methods alone will not be able to overcome the current Eurocentric biases in GWAS. Broadening the sample diversity in genomic research to fully characterize the genetic architecture and understand the genetic and nongenetic contributions to human complex traits and diseases across global populations is crucial to further improve the prediction accuracy of PRS in diverse populations.

## Online content

Any methods, additional references, Nature Research reporting summaries, source data, extended data, supplementary information, acknowledgements, peer review information; details of author contributions and competing interests; and statements of data and code availability are available at <https://doi.org/10.1038/s41588-022-01054-7>.

Received: 21 December 2020; Accepted: 16 March 2022;

Published online: 5 May 2022

## References

- Khera, A. V. et al. Genome-wide polygenic scores for common diseases identify individuals with risk equivalent to monogenic mutations. *Nat. Genet.* **50**, 1219–1224 (2018).
- Khera, A. V. et al. Polygenic prediction of weight and obesity trajectories from birth to adulthood. *Cell* **177**, 587–596.e9 (2019).
- Torkamani, A., Wineinger, N. E. & Topol, E. J. The personal and clinical utility of polygenic risk scores. *Nat. Rev. Genet.* **19**, 581–590 (2018).
- Chatterjee, N., Shi, J. & Garcia-Closas, M. Developing and evaluating polygenic risk prediction models for stratified disease prevention. *Nat. Rev. Genet.* **17**, 392–406 (2016).
- Zheutlin, A. B. et al. Penetrance and pleiotropy of polygenic risk scores for schizophrenia in 106,160 patients across four health care systems. *Am. J. Psychiatry* **176**, 846–855 (2019).
- Lambert, S. A., Abraham, G. & Inouye, M. Towards clinical utility of polygenic risk scores. *Hum. Mol. Genet.* **28**, R133–R142 (2019).
- Martin, A. R. et al. Clinical use of current polygenic risk scores may exacerbate health disparities. *Nat. Genet.* **51**, 584–591 (2019).
- Martin, A. R. et al. Human demographic history impacts genetic risk prediction across diverse populations. *Am. J. Hum. Genet.* **100**, 635–649 (2017).
- Wang, Y. et al. Theoretical and empirical quantification of the accuracy of polygenic scores in ancestry divergent populations. *Nat. Commun.* **11**, 3865 (2020).
- Duncan, L. et al. Analysis of polygenic risk score usage and performance in diverse human populations. *Nat. Commun.* **10**, 1–9 (2019).
- Popejoy, A. B. & Fullerton, S. M. Genomics is failing on diversity. *Nature* **538**, 161–164 (2016).
- Sirugo, G., Williams, S. M. & Tishkoff, S. A. The missing diversity in human genetic studies. *Cell* **177**, 26–31 (2019).
- Hindorff, L. A. et al. Prioritizing diversity in human genomics research. *Nat. Rev. Genet.* **19**, 175–185 (2018).
- Peterson, R. E. et al. Genome-wide association studies in ancestrally diverse populations: opportunities, methods, pitfalls, and recommendations. *Cell* **179**, 589–603 (2019).
- Lam, M. et al. Comparative genetic architectures of schizophrenia in East Asian and European populations. *Nat. Genet.* **51**, 1670–1678 (2019).
- Brown, B. C., Ye, C. J., Price, A. L. & Zaitlen, N. Transthetic genetic-correlation estimates from summary statistics. *Am. J. Hum. Genet.* **99**, 76–88 (2016).
- Shi, H. et al. Localizing components of shared transthetic genetic architecture of complex traits from GWAS summary data. *Am. J. Hum. Genet.* **106**, 805–817 (2020).
- Shi, H. et al. Population-specific causal disease effect sizes in functionally important regions impacted by selection. *Nat. Commun.* **12**, 1098–15 (2021).
- Ge, T., Chen, C.-Y., Ni, Y., Feng, Y.-C. A. & Smoller, J. W. Polygenic prediction via Bayesian regression and continuous shrinkage priors. *Nat. Commun.* **10**, 1776 (2019).
- Privé, F., Arbel, J. & Vilhjalmsson, B. J. LDpred2: better, faster, stronger. *Bioinformatics* **36**, 5424–5431 (2020).
- Vilhjalmsson, B. J. et al. Modeling linkage disequilibrium increases accuracy of polygenic risk scores. *Am. J. Hum. Genet.* **97**, 576–592 (2015).
- Lloyd-Jones, L. R. et al. Improved polygenic prediction by Bayesian multiple regression on summary statistics. *Nat. Commun.* **10**, 5086 (2019).
- Mak, T. S. H., Porsch, R. M., Choi, S. W., Zhou, X. & Sham, P. C. Polygenic scores via penalized regression on summary statistics. *Genet. Epidemiol.* **41**, 469–480 (2017).
- Coram, M. A., Fang, H., Candille, S. I., Assimes, T. L. & Tang, H. Leveraging multi-ethnic evidence for risk assessment of quantitative traits in minority populations. *Am. J. Hum. Genet.* **101**, 218–226 (2017).
- Grinde, K. E. et al. Generalizing polygenic risk scores from Europeans to Hispanics/Latinos. *Genet. Epidemiol.* **43**, 50–62 (2019).
- Marquez-Luna, C., Loh, P.-R., South Asian Type 2 Diabetes (SAT2D) Consortium, SIGMA Type 2 Diabetes Consortium, & Price, A. L. Multiethnic polygenic risk scores improve risk prediction in diverse populations. *Genet. Epidemiol.* **41**, 811–823 (2017).
- Weissbrod, O. et al. Leveraging fine-mapping and multipopulation training data to improve cross-population polygenic risk scores. *Nat. Genet.* **54**, 450–458 (2022).
- Sudlow, C. et al. UK Biobank: an open access resource for identifying the causes of a wide range of complex diseases of middle and old age. *PLoS Med.* **12**, e1001779 (2015).
- Kanai, M. et al. Genetic analysis of quantitative traits in the Japanese population links cell types to complex human diseases. *Nat. Genet.* **50**, 390–400 (2018).
- Sakaue, S. et al. A cross-population atlas of genetic associations for 220 human phenotypes. *Nat. Genet.* **53**, 1415–1424 (2021).
- Wojcik, G. L. et al. Genetic analyses of diverse populations improves discovery for complex traits. *Nature* **570**, 514–518 (2019).
- Chen, C.-Y. et al. Analysis across Taiwan Biobank, Biobank Japan and UK Biobank identifies hundreds of novel loci for 36 quantitative traits. Preprint at medRxiv <https://doi.org/10.1101/2021.04.12.21255236> (2021).
- Feng, Y.-C. A. et al. Taiwan Biobank: a rich biomedical research database of the Taiwanese population. Preprint at medRxiv <https://doi.org/10.1101/2021.12.21.21268159> (2021).
- Schizophrenia Working Group of the Psychiatric Genomics Consortium. Biological insights from 108 schizophrenia-associated genetic loci. *Nature* **511**, 421–427 (2014).
- International Schizophrenia Consortium et al. Common polygenic variation contributes to risk of schizophrenia and bipolar disorder. *Nature* **460**, 748–752 (2009).
- 1000 Genomes Project Consortium et al. A global reference for human genetic variation. *Nature* **526**, 68–74 (2015).
- Su, Z., Marchini, J. & Donnelly, P. HAPGEN2: simulation of multiple disease SNPs. *Bioinformatics* **27**, 2304–2305 (2011).
- Gelman, A. & Rubin, D. B. Inference from iterative simulation using multiple sequences. *Stat. Sci.* **7**, 457–472 (1992).

39. Ge, T. et al. Validation of a trans-ancestry polygenic risk score for type 2 diabetes in diverse populations. Preprint at *medRxiv* <https://doi.org/10.1101/2021.09.11.21263413> (2021).
40. Majara, L. et al. Low generalizability of polygenic scores in African populations due to genetic and environmental diversity. Preprint at *bioRxiv* <https://doi.org/10.1101/2021.01.12.426453> (2021).
41. Atkinson, E. G. et al. Tractor uses local ancestry to enable the inclusion of admixed individuals in GWAS and to boost power. *Nat. Genet.* **53**, 195–204 (2021).
42. Maples, B. K., Gravel, S., Kenny, E. E. & Bustamante, C. D. RFMix: a discriminative modeling approach for rapid and robust local-ancestry inference. *Am. J. Hum. Genet.* **93**, 278–288 (2013).

**Publisher's note** Springer Nature remains neutral with regard to jurisdictional claims in published maps and institutional affiliations.

© The Author(s), under exclusive licence to Springer Nature America, Inc. 2022, corrected publication 2022

## Stanley Global Asia Initiatives

**Yong Min Ahn<sup>18</sup>, Kazufumi Akiyama<sup>19</sup>, Makoto Arai<sup>20</sup>, Ji Hyun Baek<sup>21</sup>, Wei J. Chen<sup>22</sup>, Young-Chul Chung<sup>23</sup>, Gang Feng<sup>24</sup>, Kumiko Fujii<sup>25</sup>, Stephen J. Glatt<sup>26,27</sup>, Zhenglin Guo<sup>1</sup>, Kyooseob Ha<sup>18</sup>, Kotaro Hattori<sup>28</sup>, Teruhiko Higuchi<sup>29</sup>, Akitoyo Hishimoto<sup>30</sup>, Kyung Sue Hong<sup>21</sup>, Yasue Horiuchi<sup>20</sup>, Hailiang Huang<sup>1,8,16,60</sup>, Hai-Gwo Hwu<sup>31</sup>, Masashi Ikeda<sup>32</sup>, Sayuri Ishiwata<sup>28</sup>, Masanari Itokawa<sup>20</sup>, Nakao Iwata<sup>32</sup>, Eun-Jeong Joo<sup>33</sup>, Rene S. Kahn<sup>34</sup>, Sung-Wan Kim<sup>35</sup>, Se Joo Kim<sup>36</sup>, Se Hyun Kim<sup>18</sup>, Makoto Kinoshita<sup>37</sup>, Hiroshi Kunugi<sup>28</sup>, Agung Kusumawardhani<sup>38</sup>, Jimmy Lee<sup>39,40</sup>, Byung Dae Lee<sup>41</sup>, Heon-Jeong Lee<sup>42</sup>, Jianjun Liu<sup>43,44</sup>, Ruize Liu<sup>1,8</sup>, Xiancang Ma<sup>45</sup>, Woojae Myung<sup>46</sup>, Shusuke Numata<sup>37</sup>, Tetsuro Ohmori<sup>37</sup>, Ikuo Otsuka<sup>30,47</sup>, Yuji Ozeki<sup>25</sup>, Shengying Qin<sup>2,60</sup>, Yunfeng Ruan<sup>1,2</sup>, Akira Sawa<sup>15</sup>, Sibylle G. Schwab<sup>48,49</sup>, Wenzhao Shi<sup>24</sup>, Kazutaka Shimoda<sup>50</sup>, Kang Sim<sup>39</sup>, Ichiro Sora<sup>30</sup>, Jinsong Tang<sup>51,52,53,54</sup>, Tomoko Toyota<sup>55</sup>, Ming Tsuang<sup>56</sup>, Dieter B. Wildenauer<sup>57</sup>, Hong-Hee Won<sup>58</sup>, Takeo Yoshikawa<sup>55</sup>, Alice Zheng<sup>1</sup> and Feng Zhu<sup>59</sup>**

<sup>18</sup>Department of Psychiatry, Seoul National University Hospital, Seoul, Korea. <sup>19</sup>Department of Biological Psychiatry and Neuroscience, Dokkyo Medical University School of Medicine, Mibu, Japan. <sup>20</sup>Department of Psychiatry and Behavioral Sciences, Tokyo Metropolitan Institute of Medical Science, Tokyo, Japan. <sup>21</sup>Department of Psychiatry, Sungkyunkwan University, Samsung Medical Center, Seoul, Korea. <sup>22</sup>Department of Psychiatry, National Taiwan University Hospital and College of Medicine, National Taiwan University, Taipei, Taiwan. <sup>23</sup>Department of Psychiatry, Chonbuk National University Medical School, Jeonbuk, Korea. <sup>24</sup>Digital China Health Technologies Corp. Ltd., Beijing, China. <sup>25</sup>Department of Psychiatry, Shiga University of Medical Science, Shiga, Japan. <sup>26</sup>Department of Psychiatry and Behavioral Sciences, SUNY Upstate Medical University, Syracuse, NY, USA. <sup>27</sup>Department of Neuroscience and Physiology, SUNY Upstate Medical University, Syracuse, NY, USA. <sup>28</sup>National Institute of Neuroscience, National Center of Neurology and Psychiatry, Tokyo, Japan. <sup>29</sup>National Center of Neurology and Psychiatry, Tokyo, Japan. <sup>30</sup>Department of Psychiatry, Kobe University Graduate School of Medicine, Kobe, Japan. <sup>31</sup>Department of Psychiatry, National Taiwan University, Taipei, Taiwan. <sup>32</sup>Department of Psychiatry, Fujita Health University School of Medicine, Toyoake, Japan. <sup>33</sup>Department of Neuropsychiatry, School of Medicine, Eulji University, Daejeon, Korea. <sup>34</sup>Department of Psychiatry, Icahn School of Medicine at Mount Sinai, New York, NY, USA. <sup>35</sup>Department of Psychiatry, Chonnam National University Medical School, Gwangju, Korea. <sup>36</sup>Department of Psychiatry, Yonsei University College of Medicine, Seoul, Korea. <sup>37</sup>Department of Psychiatry, Institute of Biomedical Sciences, Tokushima University Graduate School, Tokushima, Japan. <sup>38</sup>Department of Psychiatry, University of Indonesia, Jakarta, Indonesia. <sup>39</sup>Institute of Mental Health, Singapore, Singapore. <sup>40</sup>Lee Kong Chian School of Medicine, Nanyang Technological University, Singapore, Singapore. <sup>41</sup>Department of Psychiatry, Pusan National University Hospital, Busan, Korea. <sup>42</sup>Department of Psychiatry, Korea University College of Medicine, Seoul, Korea. <sup>43</sup>Genome Institute of Singapore, A\*STAR, Singapore, Singapore. <sup>44</sup>Yong Loo Lin School of Medicine, National University of Singapore, Singapore, Singapore. <sup>45</sup>Department of Psychiatry, The First Affiliated Hospital of Xi'an Jiaotong University, Xi'an, China. <sup>46</sup>Department of Psychiatry, Seoul National University Bundang Hospital, Seongnam, Korea. <sup>47</sup>Laboratory for Statistical Analysis, RIKEN Center for Integrative Medical Sciences, Yokohama, Japan. <sup>48</sup>School of Chemistry and Molecular Bioscience, University of Wollongong, Wollongong, Australia. <sup>49</sup>Illawarra Health and Medical Research Institute, Wollongong, Australia. <sup>50</sup>Department of Psychiatry, Dokkyo Medical University School of Medicine, Mibu, Japan. <sup>51</sup>Department of Psychiatry, Sir Run Run Shaw Hospital, Zhejiang University School of Medicine, Hangzhou, Zhejiang, China. <sup>52</sup>Key Laboratory of Medical Neurobiology of Zhejiang Province, Hangzhou, Zhejiang, China. <sup>53</sup>Department of Psychiatry, the Second Xiangya Hospital, Central South University, Changsha, Hunan, China. <sup>54</sup>National Clinical Research Center on Mental Disorders, Changsha, Hunan, China. <sup>55</sup>Laboratory for Molecular Psychiatry, RIKEN Center for Brain Science, Wako, Japan. <sup>56</sup>Department of Psychiatry, University of California San Diego, San Diego, CA, USA. <sup>57</sup>University of Western Australia, Perth, Australia. <sup>58</sup>Samsung Advanced Institute for Health Sciences and Technology (SAIHST), Sungkyunkwan University, Samsung Medical Center, Seoul, Korea. <sup>59</sup>Center for Translational Medicine, The First Affiliated Hospital of Xi'an Jiaotong University, Xi'an, China.

## Methods

**PRS-CSx.** PRS-CSx is an extension of PRS-CS<sup>19</sup>, which enables the integration of GWAS summary statistics from multiple populations to improve cross-population polygenic prediction. Consider the following Bayesian high-dimensional linear regression model for  $K$  populations:

$$\mathbf{y}_k = \mathbf{X}_k \boldsymbol{\beta}_k + \boldsymbol{\epsilon}_k, \boldsymbol{\epsilon}_k \sim MVN\left(0, \sigma_k^2 \mathbf{I}\right), \pi\left(\sigma_k^2\right) \propto \sigma_k^{-2}, k = 1, 2, \dots, K,$$

where, for each population  $k$ ,  $\mathbf{y}_k$  is a vector of standardized phenotypes (zero mean and unit variance) from  $N_k$  individuals,  $\mathbf{X}_k$  is an  $N_k \times M_k$  matrix of standardized genotypes (each column has zero mean and unit variance),  $\boldsymbol{\beta}_k$  is a vector of SNP effect sizes,  $\boldsymbol{\epsilon}_k$  is a vector of normally distributed nongenetic effects with variance  $\sigma_k^2$  for which we assign a noninformative scale-invariant Jeffreys prior, and  $\mathbf{I}$  is an identity matrix. We use  $j = 1, 2, \dots, M$  to index the  $M$  unique SNPs across populations. For SNP  $j$  in population  $k$ , we place a continuous shrinkage prior on its effect size  $\beta_{jk}$ , which can be represented as global-local scale mixtures of normals:

$$\beta_{jk} \sim N\left(0, \frac{\sigma_k^2}{N_k} \psi_j\right), \psi_j \sim \text{Gamma}(a, \delta_j), \delta_j \sim \text{Gamma}(b, \phi),$$

where  $\phi$  is a global shrinkage parameter shared across all SNPs that models the overall sparseness of the genetic architecture, and  $\psi_j$  is a local, SNP-specific shrinkage parameter that is adaptive to marginal GWAS associations. By assigning a gamma-gamma hierarchical prior on  $\psi_j$  (specifically, the Strawderman-Berger prior with  $a = 1$  and  $b = 1/2$  in this work), the marginal prior density of  $\beta_{jk}$  has a sizable amount of mass near zero to impose strong shrinkage on small noisy signals, and, in the meantime, heavy Cauchy-like tails to avoid over-shrinkage of truly nonzero effects.

We note that, when SNP  $j$  is available in multiple GWAS summary statistics, the continuous shrinkage prior is shared across populations (that is, both  $\phi$  and  $\psi_j$  do not depend on  $k$ ), enabling information sharing between summary statistics while allowing for varying SNP effect sizes across populations to retain modeling flexibility. More specifically, given the variance parameters  $\sigma_k^2$ ,  $\phi$  and  $\psi_j$ , and the marginal least squares estimates of the SNP effect sizes in population  $k$ ,  $\hat{\boldsymbol{\beta}}_k = \mathbf{X}_k^T \mathbf{y}_k / N_k$ , the posterior mean of  $\boldsymbol{\beta}_k$  is

$$E\left[\boldsymbol{\beta}_k | \hat{\boldsymbol{\beta}}_k\right] = (\mathbf{D}_k + \Psi^{-1})^{-1} \hat{\boldsymbol{\beta}}_k$$

where  $\mathbf{D}_k = \mathbf{X}_k^T \mathbf{X}_k / N_k$  is the LD matrix for population  $k$ , and  $\Psi = \text{diag}\{\psi_1, \psi_2, \dots, \psi_M\}$  is a diagonal matrix (Supplementary Note). It can be seen that  $\Psi$  does not depend on  $k$  and thus the amount of shrinkage applied to each SNP is shared across populations. Meanwhile, population-specific LD patterns are explicitly modeled via the LD matrix  $\mathbf{D}_k$ .

Given the summary statistics and ancestry-matched LD reference panel for each discovery sample, the PRS-CSx model can be fitted using a Gibbs sampler with block update of posterior SNP effect sizes, without the need to access individual-level data (Supplementary Note). Monomorphic or rare variants not present in the GWAS summary statistics or population-specific LD reference panel of population A are not included in the construction of PRS for population A. If a SNP is present in population A but is monomorphic or rare in other populations, its effect size is not coupled across populations in posterior inference but the SNP is included in the PRS of population A such that population-specific associations can be captured (Fig. 1). In the extreme, unlikely scenario where there is no overlapping SNP between input GWAS summary statistics, PRS-CSx reduces to applying PRS-CS separately to each discovery GWAS. PRS-CSx inherits many features from PRS-CS, including robustness to varying genetic architectures, multivariate modeling of population-specific LD patterns, and computational efficiency. In this work, we used precalculated 1KG Phase 3 LD reference panels<sup>43</sup> for EUR, EAS, AFR and AMR populations, which were constructed for HapMap3 variants with MAF > 1%. We recommend using  $1,000 \times K$  Markov Chain Monte Carlo (MCMC) iterations with the first  $500 \times K$  steps as burn-in in Gibbs sampling, where  $K$  is the number of discovery populations, reflecting the growing number of unknown parameters with the number of discovery GWAS jointly modeled. For a fixed global shrinkage parameter  $\phi$ , PRS-CSx returns posterior SNP effect size estimates for each discovery population, which can be used to calculate  $K$  population-specific PRS in the target sample. For each  $\phi$  value, we fitted a linear (or logistic) regression of the z-scored PRS (one for each discovery population) in the validation dataset:

$$\mathbf{y} \sim w_{\phi,1} \text{PRS}_{\phi,1} + w_{\phi,2} \text{PRS}_{\phi,2} + \dots + w_{\phi,K} \text{PRS}_{\phi,K},$$

where  $\mathbf{y}$  is the trait of interest,  $\text{PRS}_{\phi,k}$  is the standardized PRS for population  $k$ , and  $w_{\phi,k}$  is the regression coefficient. We screened four different  $\phi$  values,  $10^{-6}$ ,  $10^{-4}$ ,  $10^{-2}$  and 1.0, in this work. The  $\phi$  value and the corresponding regression coefficients for the linear combination of PRS that maximized the  $R^2$  in the validation dataset were used in the testing dataset to calculate the final PRS:

$$\text{PRS} = \hat{w}_{\phi,1} \text{PRS}_{\phi,1} + \hat{w}_{\phi,2} \text{PRS}_{\phi,2} + \dots + \hat{w}_{\phi,K} \text{PRS}_{\phi,K}.$$

**Alternative PRS construction methods.** *P* value thresholding, LD-informed pruning and *P* value thresholding (PT)<sup>35</sup> selects clumped SNPs of a certain statistical significance to be included in the PRS calculation. We performed PT using PRSice-2 (ref. <sup>44</sup>) with the default parameter settings: the clumping was performed with a radius of 250 kb and an  $r^2$  threshold of 0.1. We used 1KG superpopulation samples (EUR, EAS, AFR or AMR) whose ancestry matched the discovery sample as the LD reference panel for clumping. The *P* value threshold among  $10^{-8}$ ,  $10^{-7}$ ,  $10^{-6}$ ,  $10^{-5}$ ,  $3 \times 10^{-5}$ ,  $10^{-4}$ ,  $3 \times 10^{-4}$ , 0.001, 0.003, 0.01, 0.03, 0.1, 0.3 and 1.0 that maximized the  $R^2$  in the validation dataset was selected, and used in the independent testing dataset to calculate the final PRS and its performance metrics.

**LDpred2.** LDpred2 (ref. <sup>20</sup>), an improved version of the LDpred algorithm<sup>21</sup>, is a Bayesian polygenic prediction method that adjusts marginal SNP effect size estimates from GWAS summary statistics to calculate the PRS. LDpred2 assigns a point-normal prior to SNP effect sizes, where the proportion of causal variants is a tunable parameter, and infers posterior effects using a Gibbs sampler. We constrained the computation to HapMap3 variants with MAF > 1%, and used 1KG superpopulation samples (EUR, EAS, AFR or AMR) whose ancestry matched the discovery sample as the LD reference panel. We ran LDpred2-grid using the genome-wide option with the full LD matrix, and tested the proportion of causal variants from a sequence of 17 values equally spaced from  $10^{-4}$  to 1.0 on the log scale. The proportion that maximized the  $R^2$  in the validation dataset was selected, and used in the independent testing dataset to calculate the final PRS and its performance metrics.

**PRS-CS.** PRS-CS<sup>19</sup> is a Bayesian polygenic prediction method that infers posterior SNP effect sizes from summary statistics using a continuous shrinkage prior, which is robust to varying genetic architectures, accurate in LD modeling and computationally efficient. PRS-CS has one hyperparameter—the global shrinkage parameter—which models the overall sparseness of the genetic architecture. We used default parameter settings and the precalculated 1KG LD reference panel (EUR, EAS, AFR or AMR) that matched the ancestry of the discovery sample, which was constructed for HapMap3 variants with MAF > 1%. The global shrinkage parameter among  $10^{-6}$ ,  $10^{-4}$ ,  $10^{-2}$  and 1.0 that maximized the  $R^2$  in the validation dataset was selected, and used in the independent testing dataset to calculate the final PRS and its performance metrics.

**PT-meta.** PT-meta applies PT to the meta-GWAS that combines all discovery summary statistics through an inverse-variance-weighted fixed-effect meta-analysis. We used the same clumping parameters and screened the same list of *P* value thresholds as the PT method. The 1KG LD reference panel (EUR, EAS, AFR or AMR) that had matched ancestry with each of the discovery samples was in turn used for clumping, producing multiple sets of clumped variants. The best combination of the LD reference panel and the *P* value threshold that maximized the  $R^2$  in the validation dataset was selected, and used in the independent testing dataset to calculate the final PRS and its performance metrics.

**PT-mult, LDpred2-mult and PRS-CS-mult.** PT-mult<sup>20</sup>, LDpred2-mult and PRS-CS-mult apply PT, LDpred2 and PRS-CS to each discovery summary statistics separately. The most predictive PRS derived from each discovery sample were then used to fit a linear regression in the validation dataset:

$$\mathbf{y} \sim w_1 \text{PRS}_1 + w_2 \text{PRS}_2 + \dots + w_K \text{PRS}_K,$$

where  $\text{PRS}_k$  is the standardized PRS for population  $k$ , and  $w_k$  is the corresponding regression coefficient. The optimal hyperparameter for each discovery sample and the estimated regression coefficients for the linear combination of standardized PRS were used in the independent testing dataset to calculate the final PRS and its performance metrics. We screened the same grid of hyperparameters for each method (that is, the *P* value threshold for PT, the proportion of causal variants for LDpred2 and the global shrinkage parameter for PRS-CS). The 1KG superpopulation samples (EUR, EAS, AFR or AMR) whose ancestry matched the discovery sample were used as the LD reference panel.

**Simulations. Genotypes.** We simulated individual-level genotypes of EUR, EAS and AFR populations using HAPGEN2 (ref. <sup>37</sup>) with ancestry-matched 1KG Phase 3 (ref. <sup>36</sup>) superpopulation samples as the reference panel. We grouped CEU, IBS, FIN, GBR and TSI into the EUR superpopulation, CDX, CHB, CHS, JPT and KHV into the EAS superpopulation, and ACB, ASW, LWK, MKK and YRI into the AFR superpopulation. To calculate the genetic map (cM) and recombination rate (cM/Mb) for each superpopulation, we downloaded the maps and rates for their constituent subpopulations (Data availability), linearly interpolated the genetic map and recombination rate at each position (Code availability), and averaged the genetic maps and recombination rates across the subpopulations in each superpopulation. We simulated 320,000 EUR samples, 100,000 EAS samples and 100,000 AFR samples, and confirmed that the allele frequencies and LD patterns of the simulated genotypes were highly similar to those of the 1KG reference panels. We note, however, that, although highly scalable, genotypes simulated by HAPGEN2 may not fully capture the complex population structure within and across ancestry groups. We saved 20,000 samples for each of the three populations

as the target dataset, which was split evenly into validation and testing datasets. The remaining samples served as the discovery dataset, which was used to produce GWAS of varying sample sizes. We constrained the simulations to 1,296,253 HapMap3 variants with MAF > 1% in at least one of the EUR, EAS and AFR populations, and removed triallelic and strand ambiguous variants.

**Phenotypes.** In our primary simulation, we randomly sampled 1% of the HapMap3 variants as causal variants. We assumed that causal variants are shared across the three populations and simulated their per-allele effect sizes using a multivariate normal distribution with the correlation between populations set to 0.7. For each population, we used a normally distributed random variable to model the nongenetic component such that the heritability was fixed at 50%. The phenotype was then generated in each population using  $y = X\beta + \epsilon$ , where  $X$  was the genotype matrix,  $\beta$  was the simulated per-allele effect size vector in which causal variants had nonzero effects (and the rest of the variants had zero effect sizes) and  $\epsilon$  was the simulated nongenetic component. The simulation was repeated 20 times. GWAS was performed on 100,000 EUR, 20,000 EAS and 20,000 AFR discovery samples, respectively, using PLINK 1.9 (ref. <sup>45</sup>).

We conducted a series of secondary simulations to assess the robustness of PRS-CSx in a wide range of settings: (1) varying polygenicity of the genetic architecture (0.1% versus 1% versus 10% of causal variants); (2) varying cross-population genetic correlations ( $r_g=0.4$  versus  $r_g=0.7$  versus  $r_g=1.0$ ); (3) varying sample sizes of the discovery GWAS (50,000 EUR + 10,000 non-EUR; 100,000 EUR + 20,000 non-EUR; 200,000 EUR + 40,000 non-EUR; 300,000 EUR + 60,000 non-EUR); (4) varying ratios of the EUR versus non-EUR GWAS sample sizes (120,000 EUR + 0 non-EUR; 100,000 EUR + 20,000 non-EUR; 80,000 EUR + 40,000 non-EUR; 60,000 EUR + 60,000 non-EUR); (5) varying SNP heritability of the simulated trait in different populations ( $h^2=0.5$  in EUR +  $h^2=0.5$  in non-EUR;  $h^2=0.5$  in EUR +  $h^2=0.25$  in non-EUR;  $h^2=0.25$  in EUR +  $h^2=0.5$  in non-EUR); (6) varying proportions of shared causal variants across populations (100% versus 70% versus 40%); (7) allele frequency and LD dependent genetic architecture: instead of sampling per-allele SNP effect sizes from a multivariate normal distribution with homogeneous variance across the genome, we assumed that the variance of SNP  $j$  in population  $k$  is proportional to  $[2f_{jk}(1-f_{jk})]^\alpha \ell_{jk}^\alpha$ , where  $f_{jk}$  and  $\ell_{jk}$  are the MAF and LD score of SNP  $j$  in population  $k$ , respectively. When  $\alpha < 0$ , variants with lower MAF and variants located in lower LD regions tend to have larger effects on the trait<sup>46–48</sup>. We used  $\alpha = -0.25$  in this set of simulations, which has been estimated empirically to reflect the relationship between effect size and allele frequency<sup>46</sup>. This  $\alpha$  value produced approximately a fourfold difference in the variance of per-allele effect size for both high-frequency versus low-frequency variants and high-LD versus low-LD variants included in the simulations; (8) varying hyperparameters in the continuous shrinkage prior ( $a=0.5, b=0.5$  versus  $a=1.0, b=0.5$  versus  $a=1.5, b=0.5$  versus  $a=1.0, b=1.0$ ).

**UKBB, BBJ, PAGE and TWB analysis.** Discovery data: we downloaded GWAS summary statistics from UKBB<sup>20</sup>, BBJ<sup>29</sup> and PAGE<sup>31</sup> (Data availability). We selected 33 quantitative traits that were available in both UKBB and BBJ, among which 14 were also available in PAGE (Supplementary Table 10). We used 1KG EUR and EAS samples as the LD reference panel for UKBB and BBJ summary statistics, respectively, when constructing PRS. The PAGE study comprised largely African American and Hispanic/Latino samples, for which we used the 1KG AMR reference panel as an approximation in the PRS analyses. UKBB target data: all UKBB target samples are unrelated UKBB individuals that are nonoverlapping and unrelated with the UKBB GWAS sample. To perform population assignment on the UKBB samples, we selected variants that are available in both 1KG and the UKBB genotyped dataset, and removed variants meeting one of the following criteria in 1KG: (1) strand ambiguous; (2) located on sex chromosomes or in long-range LD regions (chr6: 25–35 Mb; chr8: 7–13 Mb); (3) call rate < 0.98; and (4) MAF < 0.05. We performed LD pruning on the remaining variants in 1KG using PLINK<sup>45</sup> (-indep-pairwise 100 50 0.2), yielding 149,501 largely independent, high-quality common variants. We then conducted PC analysis using these LD-pruned SNPs in 1KG samples, and projected SNP loadings onto UKBB samples with the scale appropriately adjusted. Using 1KG as the reference, we trained a random forest model to predict the five superpopulation labels (AFR, AMR, EAS, EUR, SAS) using the top six PCs, and applied the trained random forest classifier to UKBB samples to predict the genetic ancestry of each UKBB participant. We retained UKBB samples that can be assigned to one of the superpopulations with a predicted probability > 90%. For each population in UKBB, we selected a set of unrelated individuals and performed sample-level quality control (QC) by removing individuals meeting one of the following criteria: (1) mismatch between self-reported and genetically inferred sex; (2) missingness or heterozygosity outliers and (3) sex chromosome aneuploidy. For the validation and testing of PRS in the EUR population, we used non-British EUR samples that are unrelated to the White British samples included in Neale Lab UKBB GWAS. Last, we converted imputed dosage data into hard coded genotypes using PLINK 2.0 with default parameters (that is, dosage was rounded to the nearest hardcall when the distance was no greater than 0.1; otherwise a missing hardcall was saved), and performed variant-level QC in each target population by removing variants meeting one of the following criteria: (1) call rate < 0.98; (2) MAF < 0.01; (3) Hardy–Weinberg

equilibrium test  $P$  value <  $10^{-10}$  and (4) imputation INFO score < 0.8. The final target dataset included 7,507 AFR, 687 AMR, 2,181 EAS, 14,085 EUR and 8,412 SAS individuals, with 12,886,200, 8,593,932, 6,506,126, 8,211,053 and 8,032,121 variants, respectively. TWB target data: The TWB<sup>32,33</sup> is a prospective cohort study of the Taiwanese population. Participants were 30–70 years old at recruitment. Among the 33 quantitative traits examined in UKBB, we identified 21 that were also available in TWB. We used 14,232 samples genotyped on the TWBv2 custom array and imputed against the 1KG samples, the same dataset used in the PRS analysis of our recent TWB quantitative trait GWAS study<sup>32</sup>, to evaluate the predictive performance of different polygenic prediction methods. Following the same sample-level and variant-level QC procedures used in the UKBB analysis, the final analytic sample included 10,149 unrelated individuals of EAS ancestry that had complete data across the 21 traits. Detailed information on the sample characteristics and collection of phenotypes can be found elsewhere<sup>32,33</sup>.

**Heritability and cross-population genetic correlation.** Heritability of each trait in UKBB, BBJ and PAGE was estimated using LD score regression<sup>49</sup> with ancestry-matched LD reference panels. We calculated the cross-population genetic correlation between UKBB, BBJ and PAGE using POPCORN<sup>16</sup> with default parameters. POPCORN requires the LD score<sup>46</sup> and cross-covariance score as the input. We used the precomputed EUR–EAS scores (available from the POPCORN website), and computed EUR–AFR and EAS–AFR scores on 1KG Phase 3 samples using the ‘compute’ function provided by POPCORN.

**Schizophrenia datasets.** Schizophrenia data used in this study is summarized in Supplementary Table 16. PGC wave 2 schizophrenia GWAS summary statistics<sup>34</sup> were used as the European discovery dataset. Except for one cohort (TMIM1), EAS samples used as discovery and target datasets were described in Lam et al<sup>15</sup>. TMIM1 was recruited from multiple university hospitals and local hospitals in Japan. Patients were diagnosed according to the Diagnostic and Statistical Manual of Mental Disorders, 4th Edition (DSM-IV) with consensus from at least two experienced psychiatrists. All patients agreed to participate in the study and provided written informed consent. The study was approved by the Institutional Review Boards of the Tokyo Metropolitan Institute of Medical Science and all affiliated institutions. DNA samples were genotyped on the Illumina Infinium Global Screening Array-24 v.1.0 (GSA) BeadChip at the Broad Institute, using standard reagents and HTS workflow procedures. GWAS QC and imputation were performed using Ricopili<sup>50</sup> with default parameters. When used as a target cohort, SNPs were further filtered by imputation INFO score < 0.9 and MAF < 0.01.

**Ethics.** Collection of the UKBB data was approved by the Research Ethics Committee of the UKBB. UKBB individual-level data used in the present work were obtained under application no. 32568. BBJ and PAGE: only publicly available GWAS summary statistics, without individual-level information, were used in this study. Collection of the TWB data was approved by the Ethics and Governance Council (EGC) of TWB and the Department of Health and Welfare, Taiwan (Wei-Shu-I-Tzu no. 1010267471). TWB obtained informed consent from all participants for research use of the collected data. Access to, and use of, TWB data in the present work was approved by the EGC of TWB (approval number: TWBR10907-05) and the Institutional Review Board of National Health Research Institutes, Taiwan (approval number: EC1090402-E). Schizophrenia GWAS summary statistics of EUR and EAS ancestries are available via the Psychiatric Genomics Consortium, and do not contain any individual-level information. The following institutions provided ethics oversight for schizophrenia East Asian samples used in this work: Samsung Medical Center, Bio-X Institutes of Shanghai Jiao Tong University, Fujita Health University, Tokyo Metropolitan Institute of Medical Science, University Medical Center Utrecht, The University of Western Australia, The University of Indonesia, RIKEN Center for Integrative Medical Sciences, Nagoya University, Osaka University, Niigata University, Chonnam National University Hospital and Mass General Brigham (Protocols 2014P001342 and 2011P002207). Informed consent and permission to share the data were obtained from all subjects, in compliance with the guidelines specified by the institutional review board of the recruiting center.

**Reporting Summary.** Further information on research design is available in the Nature Research Reporting Summary linked to this article.

## Data availability

Publicly available data are available from the following sites: 1KG Phase 3 reference panels: [https://mathgen.stats.ox.ac.uk/impute/1000GP\\_Phase3.html](https://mathgen.stats.ox.ac.uk/impute/1000GP_Phase3.html); Genetic map for each subpopulation: [ftp://1000genomes.ebi.ac.uk/vol1/ftp/technical/working/20130507\\_omni\\_recombination\\_rates](ftp://1000genomes.ebi.ac.uk/vol1/ftp/technical/working/20130507_omni_recombination_rates); UKBB summary statistics: <http://www.nealelab.is/uk-biobank> ('GWAS round 2' was used in this study); BBJ summary statistics were downloaded from PheWeb: <https://pheweb.jp>; PAGE summary statistics were downloaded from the GWAS Catalog: <https://www.ebi.ac.uk/gwas/downloads/summary-statistics>; PGC wave 2 schizophrenia GWAS (49 EUR cohorts): <https://www.med.unc.edu/pgc/download-results/>; leave-one-out schizophrenia EAS summary statistics are available upon request to the Schizophrenia Working Group of the PGC (<https://www.med.unc.edu/>

[pgc/pgc-workgroups/schizophrenia/](https://pgc.broadinstitute.org/pgc-workgroups/schizophrenia/)). These leave-one-out summary statistics are under controlled access per the data use limitation imposed by compliance, participant consent and/or national laws. Application to access such data requires a short research proposal that will go through review and approval process of the PGC. This process takes 2 weeks. Individual-level schizophrenia data of East Asian ancestry are available upon application to the Stanley Global Asia Initiatives: SGAI@broadinstitute.org. These data must be under controlled access due to the data use limitation imposed by the compliance, participant consent and national laws. Application to access such data requires a short research proposal that will be reviewed by principal investigator of the constituent study and, if necessary, by the respective ethic committee. The principal investigator review process takes 2 weeks. TWB data used in this study contain protected health information and are thus under controlled access. Application to access such data can be made to the TWB ([https://www.twbiobank.org.tw/new\\_web\\_en/](https://www.twbiobank.org.tw/new_web_en/)). Posterior SNP effect size estimates generated by PRS-CSx for the traits examined in this work: <https://github.com/getian107/PRScsx>.

## Code availability

The code used in this study is available from the following websites: PRS-CSx: <https://github.com/getian107/PRScsx> (<https://doi.org/10.5281/zenodo.5893746>); PRS-CS: <https://github.com/getian107/PRScs> (<https://doi.org/10.5281/zenodo.5893748>); LDpred2: <https://privefl.github.io/bigsnp/articles/LDpred2>; PRSice-2: <https://www.prstice.info>; HAPGEN2: [https://mathgen.stats.ox.ac.uk/genetics\\_software/hapgen/hapgen2.html](https://mathgen.stats.ox.ac.uk/genetics_software/hapgen/hapgen2.html); PLINK 1.9: <https://www.cog-genomics.org/plink/>; PLINK 2.0: <https://www.cog-genomics.org/plink/2.0/>; LD score regression: <https://github.com/bulik/ldsc>; POPCORN: <https://github.com/brielin/Popcorn>; Interpolation of genetic maps: <https://github.com/joepickrell/1000-genomes-genetic-maps>; Population assignment: <https://github.com/Annefeng/PBK-QC-pipeline>.

## References

43. Berisa, T. & Pickrell, J. K. Approximately independent linkage disequilibrium blocks in human populations. *Bioinformatics* **32**, 283–285 (2016).
44. Choi, S. W. & O'Reilly, P. F. PRSice-2: Polygenic Risk Score software for biobank-scale data. *GigaScience* **8**, 2091 (2019).
45. Chang, C. C. et al. Second-generation PLINK: rising to the challenge of larger and richer datasets. *GigaScience* **4**, 7 (2015).
46. Zeng, J. et al. Signatures of negative selection in the genetic architecture of human complex traits. *Nat. Genet.* **360**, 1411–1753 (2018).
47. Gazal, S. et al. Linkage disequilibrium-dependent architecture of human complex traits shows action of negative selection. *Nat. Genet.* **49**, 1421–1427 (2017).
48. Speed, D., Holmes, J. & Balding, D. J. Evaluating and improving heritability models using summary statistics. *Nat. Genet.* **52**, 458–462 (2020).
49. Bulik-Sullivan, B. K. et al. LD Score regression distinguishes confounding from polygenicity in genome-wide association studies. *Nat. Genet.* **47**, 291–295 (2015).
50. Lam, M. et al. RICOPILI: Rapid Imputation for COnsortias PIpeLine. *Bioinformatics* **36**, 930–933 (2020).

## Acknowledgements

We thank B. Neale, M. Daly, R. Do and A. Bloemendal for helpful discussions. We thank the Neale Laboratory and BBJ for releasing the genome-wide association summary statistics from UKBB and BBJ. Individual-level phenotypes and genotypes for UKBB samples were obtained under application 32568. We thank the Schizophrenia Working Group of the PGC for providing the GWAS summary statistics for schizophrenia. T.G. is supported by National Institute on Aging (NIA) K99/R00AG054573, National Human Genome Research Institute (NHGRI) U01HG008685 and NHGRI U01HG011723. H.H. acknowledges supports from National Institute of Diabetes and Digestive and Kidney Diseases (NIDDK) K01DK114379, National Institute of Mental Health (NIMH) U01MH109539, Brain and Behavior Research Foundation Young Investigator Grant (28450), the Zhengxu and Ying He Foundation, and the Stanley Center for Psychiatric Research. L.H. and S.Q. are supported by Shanghai Municipal Science and Technology Major Project (2017SHZDZX01). A.R.M. is supported by NIMH K99/R00MH117229. A.S. is supported by NIMH P50MH094268. Y.A.F. is supported by the 'National Taiwan University Higher Education Sprout Project (NTU-110L8810)' within the framework of the Higher Education Sprout Project by the Ministry of Education (MOE) in Taiwan. Y.F.L. is supported by the National Health Research Institutes (NP-109-PP-09), and the Ministry of Science and Technology (109-2314-B-400-017) of Taiwan.

## Author contributions

H.H. and T.G. designed the project; T.G. developed the statistical methods and programmed the code for PRS-CSx. Y.R. and T.G. conducted simulation studies. Y.R. and T.G. performed the analysis in the UK Biobank; Y.-F.L. performed the analysis in the Taiwan Biobank. Y.R. performed the analysis in the schizophrenia cohorts. Y.-C.A.F. assigned the UKBB samples into superpopulation groups. C.-Y.C. provided critical suggestions for the study design. M.L. took part in the testing of the code and preprocessed schizophrenia East Asian cohorts. Z.G., L.H., A.S. and S.Q. contributed to the generation and preprocessing of schizophrenia East Asian data. Y.R., H.H. and T.G. wrote the manuscript; Y.-C.A.F., C.-Y.C. and A.R.M. provided critical revision for the manuscript. All the authors reviewed and approved the final version of the manuscript.

## Competing interests

C.Y.C. is an employee of Biogen. The other authors declare no competing interests.

## Additional information

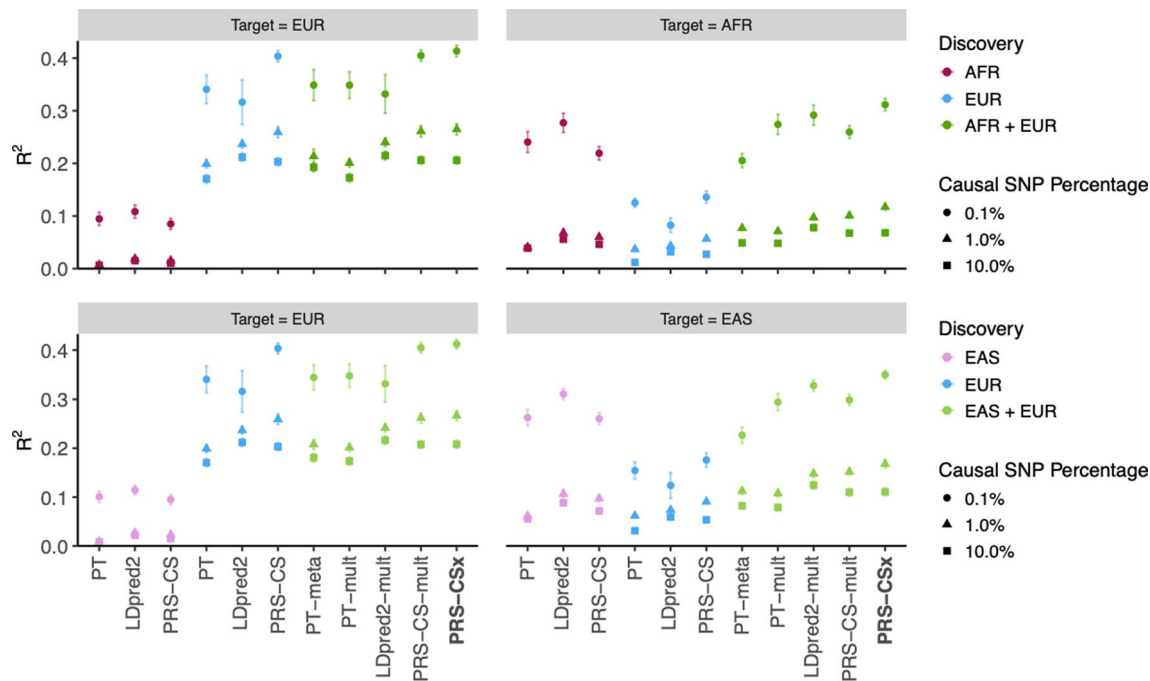
**Extended data** is available for this paper at <https://doi.org/10.1038/s41588-022-01054-7>.

**Supplementary information** The online version contains supplementary material available at <https://doi.org/10.1038/s41588-022-01054-7>.

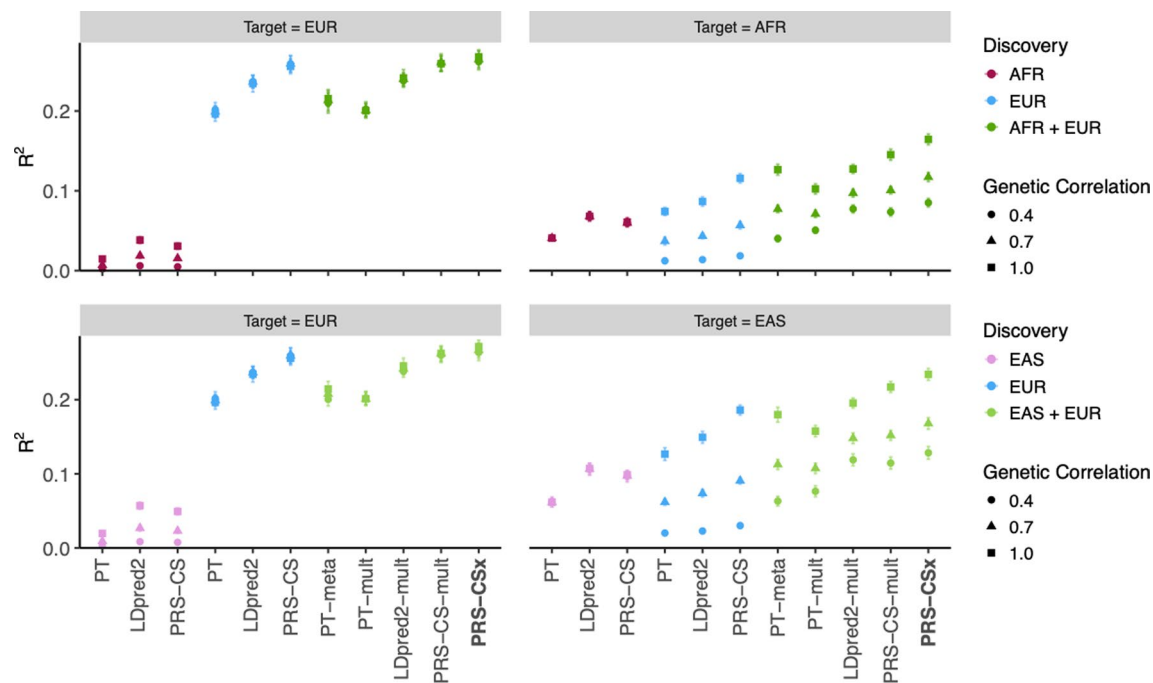
**Correspondence and requests for materials** should be addressed to Shengying Qin, Hailiang Huang or Tian Ge.

**Peer review information** *Nature Genetics* thanks Yixuan Ye, Shing Wan Choi and the other, anonymous, reviewer(s) for their contribution to the peer review of this work. Peer reviewer reports are available.

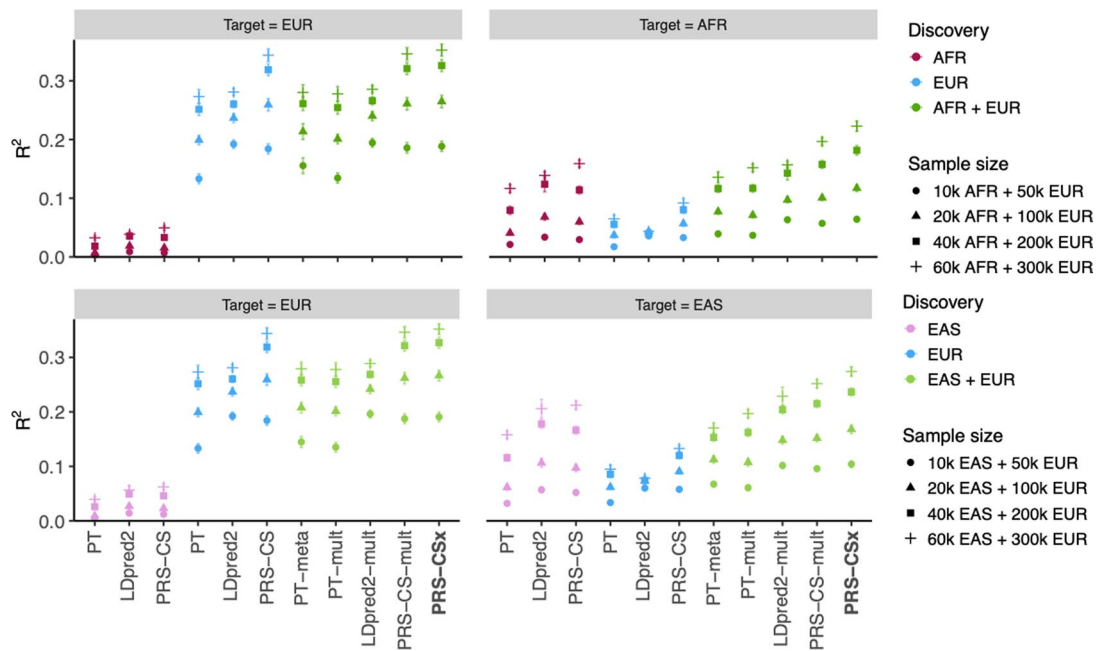
**Reprints and permissions information** is available at [www.nature.com/reprints](http://www.nature.com/reprints).



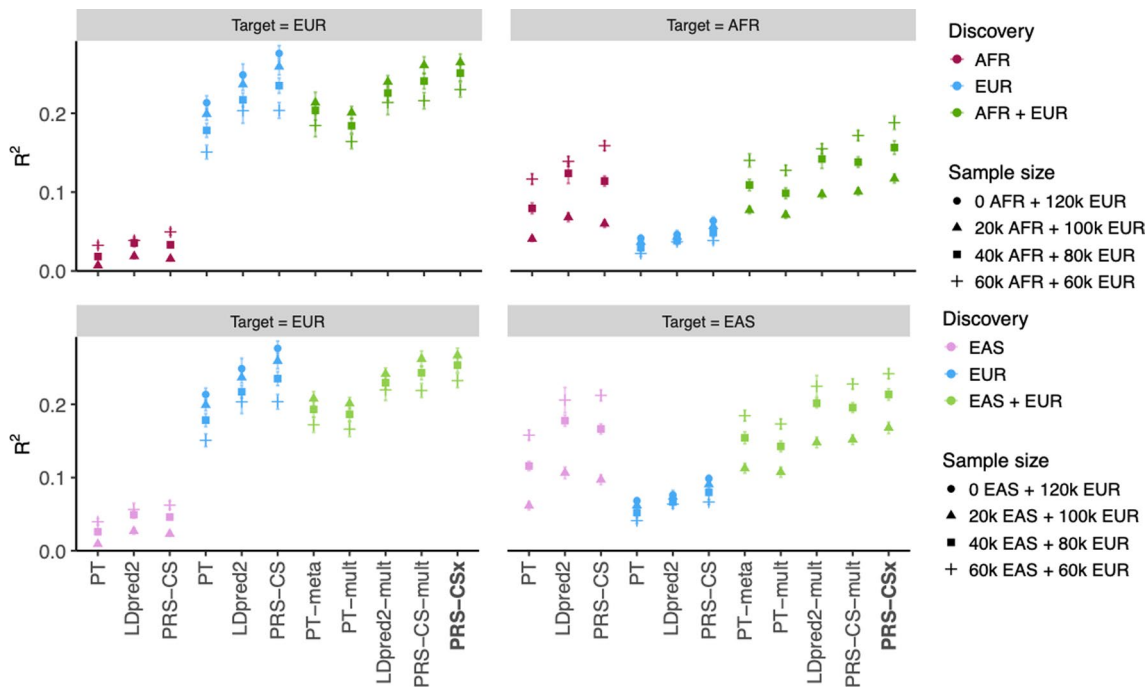
**Extended Data Fig. 1 | Prediction accuracy of different polygenic prediction methods across different genetic architectures.** Phenotypes were simulated using 0.1%, 1% or 10% of randomly sampled causal variants (shared across populations), a cross-population genetic correlation of 0.7, and SNP heritability of 50%. PRS were trained using 100 K EUR samples and 20 K non-EUR (EAS or AFR) samples. Numerical results are reported in Supplementary Table 2.



**Extended Data Fig. 2 | Prediction accuracy of different polygenic prediction methods across different cross-population genetic correlations.** Phenotypes were simulated using 1% of randomly sampled causal variants (shared across populations), a cross-population genetic correlation of 0.4, 0.7 or 1.0, and SNP heritability of 50%. PRS were trained using 100 K EUR samples and 20 K non-EUR (EAS or AFR) samples. Numerical results are reported in Supplementary Table 3.

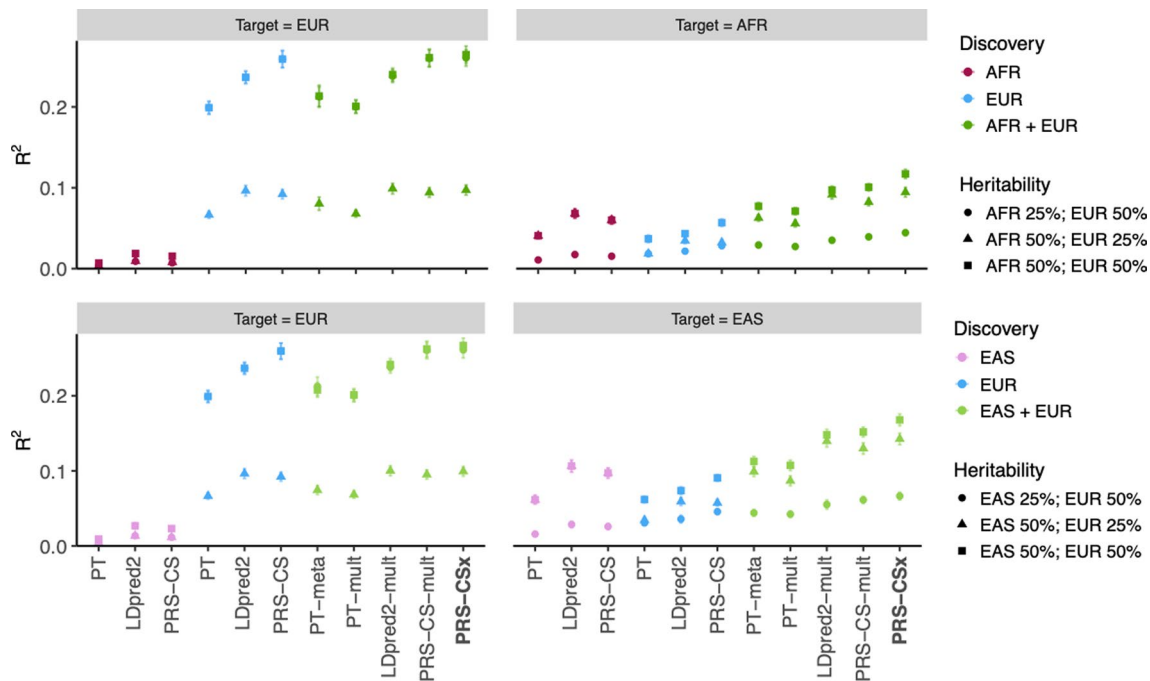


**Extended Data Fig. 3 | Prediction accuracy of different polygenic prediction methods across different discovery GWAS sample sizes.** Phenotypes were simulated using 1% of randomly sampled causal variants (shared across populations), a cross-population genetic correlation of 0.7, and SNP heritability of 50%. PRS were trained using 50 K EUR and 10 K non-EUR (EAS or AFR) samples, 100 K EUR and 20 K non-EUR samples, 200 K EUR and 40 K non-EUR samples, or 300 K EUR and 60 K non-EUR samples. Numerical results are reported in Supplementary Table 4.

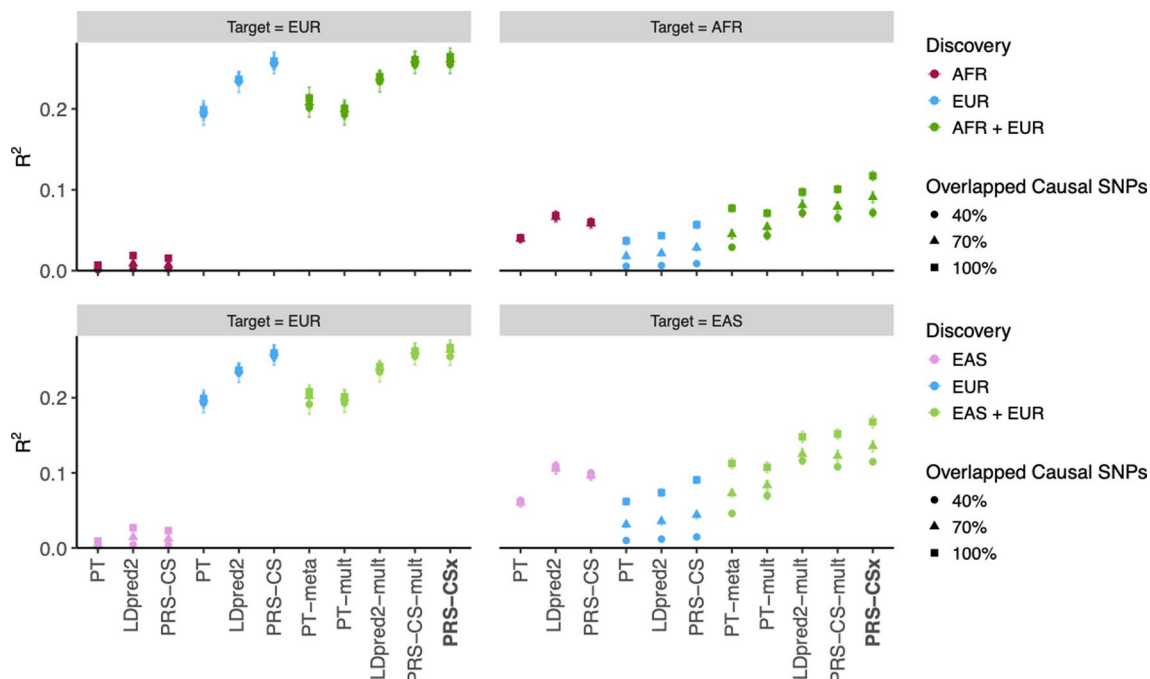


**Extended Data Fig. 4 | Prediction accuracy of different polygenic prediction methods across different ratios of EUR vs. non-EUR GWAS sample sizes.**

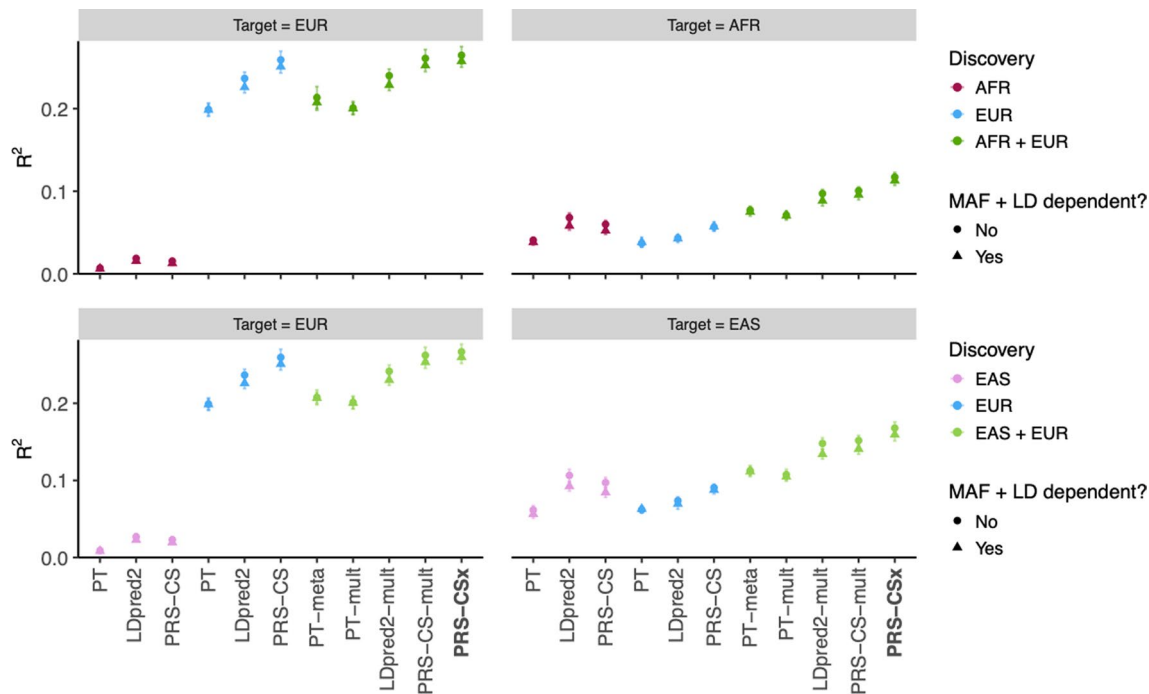
Phenotypes were simulated using 1% of randomly sampled causal variants (shared across populations), a cross-population genetic correlation of 0.7, and SNP heritability of 50%. PRS were trained using 120 K EUR samples without non-EUR samples, 100 K EUR and 20 K non-EUR (EAS or AFR) samples, 80 K EUR and 40 K non-EUR samples, or 60 K EUR and 60 K non-EUR samples. Numerical results are reported in Supplementary Table 5.



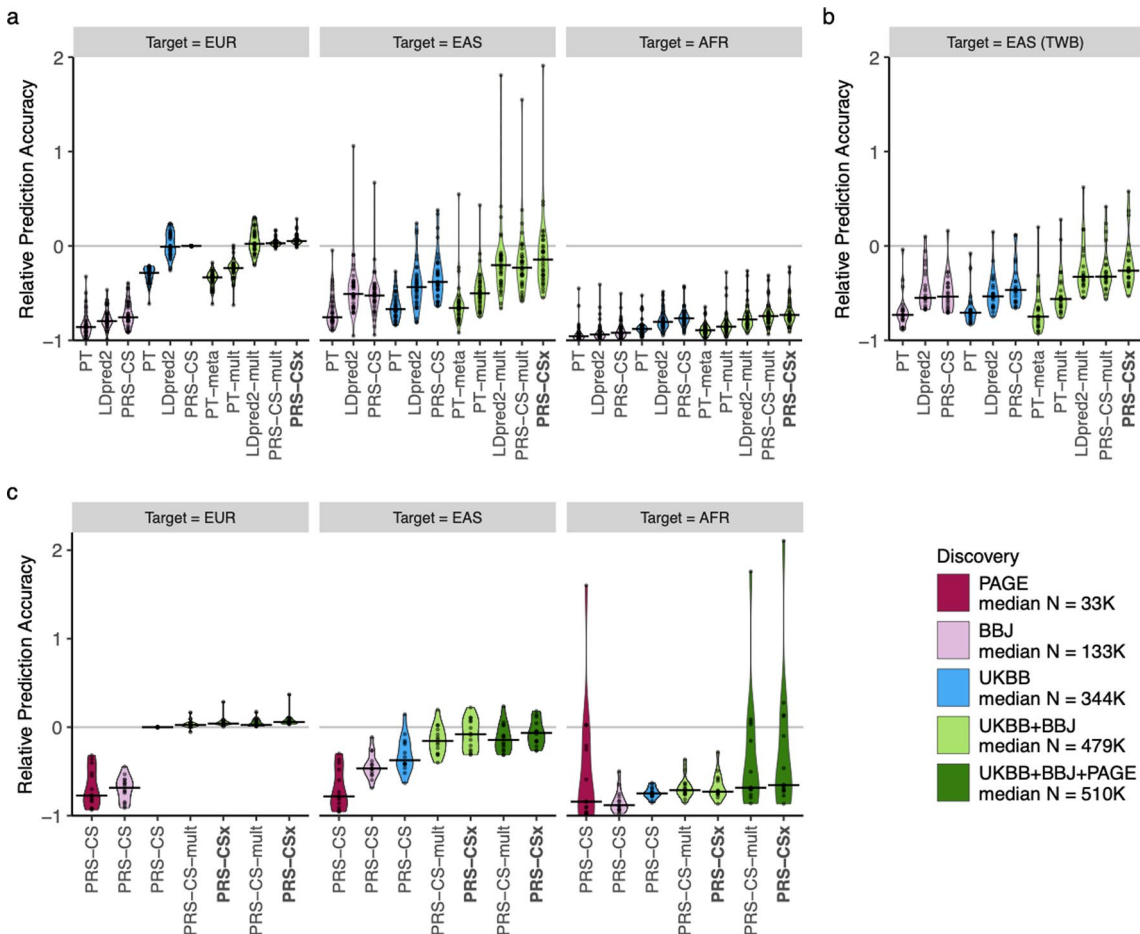
**Extended Data Fig. 5 | Prediction accuracy of different polygenic prediction methods across different SNP heritability.** Phenotypes were simulated using 1% of randomly sampled causal variants (shared across populations) and a cross-population genetic correlation of 0.7. SNP heritability was fixed at 50% in each population, 50% in the EUR population and 25% in the non-EUR population, or 25% in the EUR population and 50% in the non-EUR population. PRS were trained using 100 K EUR samples and 20 K non-EUR (EAS or AFR) samples. Numerical results are reported in Supplementary Table 6.



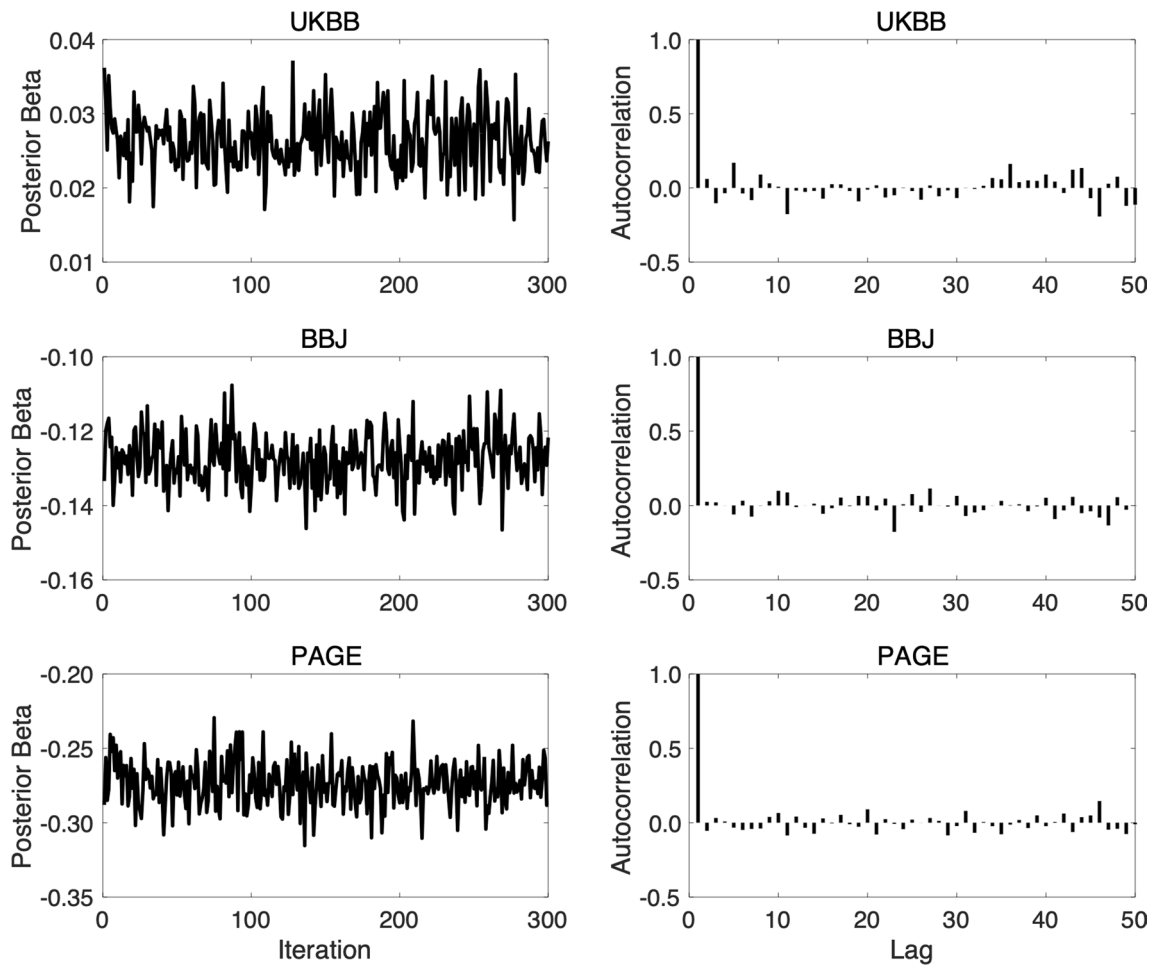
**Extended Data Fig. 6 | Prediction accuracy of different polygenic prediction methods across different proportions of shared causal variants between populations.** Phenotypes were simulated using 1% of randomly sampled causal variants. 100%, 70% or 40% of the causal variants were shared across populations. Shared causal variants had a cross-population genetic correlation of 0.7. SNP heritability was fixed at 50%. PRS were trained using 100 K EUR samples and 20 K non-EUR (EAS or AFR) samples. Numerical results are reported in Supplementary Table 7.



**Extended Data Fig. 7 | Prediction accuracy of different polygenic prediction methods when SNP effect sizes are minor allele frequency (MAF) and linkage disequilibrium (LD) dependent.** Phenotypes were simulated using 1% of randomly sampled causal variants (shared across populations), a cross-population genetic correlation of 0.7, and SNP heritability of 50%. SNP effect sizes were dependent on MAF and LD scores such that SNPs with lower MAF and located in lower LD regions tended to have larger effect sizes. PRS were trained using 100 K EUR samples and 20 K non-EUR (EAS or AFR) samples. Numerical results are reported in Supplementary Table 8.



**Extended Data Fig. 8 | Relative prediction accuracy for quantitative traits across target populations.** Relative prediction performance for single-discovery and multi-discovery PRS construction methods using discovery GWAS summary statistics **a**, from UKBB and BBJ, across 33 traits, in different UKBB target populations (EUR, EAS and AFR); **b**, from UKBB and BBJ, across 21 traits, in the Taiwan Biobank (TWB); **c**, from UKBB, BBJ and PAGE, across 14 traits, in different UKBB target populations (EUR, EAS and AFR). Each data point shows the relative increase of prediction performance, defined as  $R^2/R^2_{\text{PRS-CS (UKBB)-EUR}} - 1$ , in which  $R^2_{\text{PRS-CS (UKBB)-EUR}}$  is the  $R^2$  of the trait in the EUR population using PRS-CS trained on the UKBB GWAS summary statistics. In UKBB target populations (panels **a** and **c**),  $R^2$  were averaged across 100 random splits of the target samples into validation and testing datasets. The crossbar indicates the median of the relative increase of predictive performance across the traits examined. 'median N' indicates the median sample size across the respective discovery GWAS.



**Extended Data Fig. 9 | Trace plots and autocorrelation functions (ACFs) for assessing the convergence and mixing of the Gibbs sampler used in PRS-CSx.** Left panels: Trace plots, after discarding the burn-in iterations and thinning the Markov chain by a factor of 5, for the posterior effects of rs7412 on low-density lipoprotein cholesterol when integrating UKBB, BBJ and PAGE GWAS summary statistics using PRS-CSx. Right panels: The autocorrelation functions (ACFs) for the traces shown on the left.

## Reporting Summary

Nature Portfolio wishes to improve the reproducibility of the work that we publish. This form provides structure for consistency and transparency in reporting. For further information on Nature Portfolio policies, see our [Editorial Policies](#) and the [Editorial Policy Checklist](#).

### Statistics

For all statistical analyses, confirm that the following items are present in the figure legend, table legend, main text, or Methods section.

n/a Confirmed

- The exact sample size ( $n$ ) for each experimental group/condition, given as a discrete number and unit of measurement
- A statement on whether measurements were taken from distinct samples or whether the same sample was measured repeatedly
- The statistical test(s) used AND whether they are one- or two-sided
  - Only common tests should be described solely by name; describe more complex techniques in the Methods section.*
- A description of all covariates tested
- A description of any assumptions or corrections, such as tests of normality and adjustment for multiple comparisons
- A full description of the statistical parameters including central tendency (e.g. means) or other basic estimates (e.g. regression coefficient) AND variation (e.g. standard deviation) or associated estimates of uncertainty (e.g. confidence intervals)
- For null hypothesis testing, the test statistic (e.g.  $F$ ,  $t$ ,  $r$ ) with confidence intervals, effect sizes, degrees of freedom and  $P$  value noted
  - Give  $P$  values as exact values whenever suitable.*
- For Bayesian analysis, information on the choice of priors and Markov chain Monte Carlo settings
- For hierarchical and complex designs, identification of the appropriate level for tests and full reporting of outcomes
- Estimates of effect sizes (e.g. Cohen's  $d$ , Pearson's  $r$ ), indicating how they were calculated

*Our web collection on [statistics for biologists](#) contains articles on many of the points above.*

### Software and code

Policy information about [availability of computer code](#)

Data collection

The software for simulating individual-level genotypes (HAPGEN2) is available at:  
[https://mathgen.stats.ox.ac.uk/genetics\\_software/hapgen/hapgen2.html](https://mathgen.stats.ox.ac.uk/genetics_software/hapgen/hapgen2.html)  
No other software was used in data collection.

Data analysis

The code for data analysis in this study is available from the following websites:  
PRS-CSx: <https://github.com/getian107/PRScsx> (29 Jul 2021 version);  
PRS-CS: <https://github.com/getian107/PRScs> (04 Jun 2021 version);  
LDpred2: <https://privetfl.github.io/bigsnpr/articles/LDpred2> (bigsnpr v1.6.1);  
PRScse2: <https://www.prscse.info> (v2.2.11.b);  
PLINK 1.90: <https://www.cog-genomics.org/plink> (beta 6.15);  
LD score regression: <https://github.com/bulik/ldsc> (v1.0.1);  
POPCORN: <https://github.com/brielin/Popcorn> (28 Aug 2019 version);  
Interpolation of genetic maps: <https://github.com/joepickrell/1000-genomes-genetic-maps> (21 Apr 2015 version);  
Population assignment: <https://github.com/Annefeng/PBK-QC-pipeline> (30 Mar 2020 version);  
Quality control and imputation for individual-level genotypes: <https://sites.google.com/a/broadinstitute.org/ricopili/> (15 Oct 2019 version).  
Gibbs sampler was coded in PRS-CSx: <https://github.com/getian107/PRScsx> (29 Jul 2021 version);

For manuscripts utilizing custom algorithms or software that are central to the research but not yet described in published literature, software must be made available to editors and reviewers. We strongly encourage code deposition in a community repository (e.g. GitHub). See the Nature Portfolio [guidelines for submitting code & software](#) for further information.

## Data

### Policy information about availability of data

All manuscripts must include a [data availability statement](#). This statement should provide the following information, where applicable:

- Accession codes, unique identifiers, or web links for publicly available datasets
- A description of any restrictions on data availability
- For clinical datasets or third party data, please ensure that the statement adheres to our [policy](#)

Publicly available data are available from the following sites:

1KG Phase 3 reference panels: [https://mathgen.stats.ox.ac.uk/impute/1000GP\\_Phase3.html](https://mathgen.stats.ox.ac.uk/impute/1000GP_Phase3.html);

Genetic map for each subpopulation: [ftp://1000genomes.ebi.ac.uk/vol1/ftp/technical/working/20130507\\_omni\\_recombination\\_rates](ftp://1000genomes.ebi.ac.uk/vol1/ftp/technical/working/20130507_omni_recombination_rates);

UKBB summary statistics: <http://www.nealelab.is/uk-biobank> ("GWAS round 2" was used in this study);

BBJ summary statistics were downloaded from PheWeb: <https://pheweb.jp/>;

PAGE summary statistics were downloaded from the GWAS Catalog: <https://www.ebi.ac.uk/gwas/downloads/summary-statistics>;

PGC wave 2 schizophrenia GWAS (49 EUR cohorts): <https://www.med.unc.edu/pgc/download-results/>;

Leave-one-out schizophrenia EAS summary statistics are available upon request to the Schizophrenia Working Group of the PGC (<https://www.med.unc.edu/pgc/pgc-workgroups/schizophrenia/>). These leave-one-out summary statistics are under controlled access per the data use limitation imposed by compliance, participant consent and/or national laws. Application to access such data requires a short research proposal that will go through PGC's review and approval process. This process takes two weeks.

Individual-level schizophrenia data of East Asian ancestry are available upon application to the Stanley Global Asia Initiatives: SGAI@broadinstitute.org. These data must be under controlled access due to the data use limitation imposed by the compliance, participant consent and national laws. Application to access such data requires a short research proposal that will be reviewed by PI of the constituent study, and if necessary, by the respective ethic committee. The PI review process takes two weeks.

Taiwan Biobank data used in this study contain protected health information and are thus under controlled access. Application to access such data can be made to the Taiwan Biobank ([https://www.twbiobank.org.tw/new\\_web\\_en/](https://www.twbiobank.org.tw/new_web_en/)).

Posterior SNP effect size estimates generated by PRS-CSx for the traits examined in this work: <https://github.com/getian107/PRScsx>.

## Field-specific reporting

Please select the one below that is the best fit for your research. If you are not sure, read the appropriate sections before making your selection.

Life sciences       Behavioural & social sciences       Ecological, evolutionary & environmental sciences

For a reference copy of the document with all sections, see [nature.com/documents/nr-reporting-summary-flat.pdf](https://nature.com/documents/nr-reporting-summary-flat.pdf)

## Life sciences study design

All studies must disclose on these points even when the disclosure is negative.

### Sample size

Simulations: Sample size of the discovery dataset was chosen to match that of a typical genome-wide association study at present (up to 300,000 EUR individuals and up to 60,000 EAS and AFR individuals) [1,2]. 20,000 EUR, EAS and AFR individuals were used as the target dataset, which was evenly split into a validation dataset and a testing dataset, comparable to other studies [3].

Quantitative trait analysis in Biobanks: We used all subjects that were available to us.

Discovery GWAS: 33 traits from UKBB (N varied from 314,916 to 360,388) and BBJ (N varied from 71,221 to 165,419); 14 traits from PAGE (N varied from 11,178 to 49,796).

Target datasets: 7,507 AFR, 687 AMR, 2,181 EAS, 14,085 EUR and 8,412 SAS UKBB individuals after sample QC; 10,149 individuals from the Taiwan Biobank (TWB) after sample QC.

Schizophrenia analysis: We used all subjects that were available to us.

Discovery GWAS: 33,640 cases and 43,456 controls of EUR ancestry; 7,856 cases and 11,562 controls of EAS ancestry; both GWAS summary statistics were available from the Psychiatric Genomics Consortium.

Validation dataset: 687 cases and 492 controls.

Testing datasets: A total of 9,416 cases and 8,708 controls across six EAS cohorts (used in a leave-one-cohort-out fashion).

1. Bycroft et al., Nature 2018
2. Wojcik et al., Nature 2019
3. Ding et al., Nature Genetics 2022

### Data exclusions

Summary statistics used in the study: no data exclusion.

Individual-level data (all steps and parameters were pre-established before the study implementation).

UKBB and TWB: We used standard variant and sample QC for the UKBB and TWB data. Specifically, we selected variants that are available in both 1KG and the UKBB/TWB genotyped dataset, and removed variants meeting one of the following criteria in 1KG: 1) strand ambiguous; 2) located on sex chromosomes or in long-range LD regions (chr6: 25-35Mb; chr8: 7-13Mb); 3) call rate <0.98; and 4) MAF <0.05. We performed

LD pruning on the remaining variants in 1KG using PLINK (--indep-pairwise 100 50 0.2). We then conducted principal component analysis using these LD-pruned SNPs in 1KG samples, and projected SNP loadings onto samples with the scale appropriately adjusted. Using 1KG as the reference, we trained a random forest model to predict the 5 super-population labels (AFR, AMR, EAS, EUR, SAS) using the top 6 PCs, and applied the trained random forest classifier to samples to predict the genetic ancestry of each participant. We retained samples that can be assigned to one of the super-populations with a predicted probability >90%. For each population, we selected a set of unrelated individuals and performed sample-level quality control (QC) by removing individuals meeting one of the following criteria: 1) mismatch between self-reported and genetically inferred sex; 2) missingness or heterozygosity outliers; and 3) sex chromosome aneuploidy. For EUR, we used non-British EUR samples that are unrelated to the White British samples included in Neale Lab UKBB GWAS. Lastly, we performed variant-level QC within each target population by removing variants meeting one of the following criteria: 1) call rate <0.98; 2) MAF <0.01; 3) Hardy-Weinberg equilibrium test p-value <10-10; and 4) imputation INFO score <0.8.

**Schizophrenia:** We performed standard variant and sample QC for the schizophrenia genetic data, using the RICOPILI pipeline (Lam et al., Bioinformatics 2019). Specifically, we 1) excluded variants with call rate below 95%; 2) excluded subjects with call rate below 98%; 3) excluded monomorphic variants; 4) excluded subjects with inbred coefficient above 0.2 and below -0.2; 5) excluded subjects with mismatch in reported sex and chromosome X computed gender; 6) excluded variants with missing rate differences greater than 2% between cases and controls; 7) subsequent to step 6, we excluded variants with call rate below 98%; and 8) excluded variants in violation of Hardy-Weinberg equilibrium ( $P < 1e-6$  for controls or  $P < 1e-10$  for cases). Additionally, we computed the identity-by-descent matrix to identify intra- and inter-dataset sample overlaps. Samples with pi-hat > 0.2 were extracted, followed by Fisher-Yates shuffle on all samples. The number of times with which each sample was related to another sample was tracked and samples that were related to more than 25 samples were removed. Lastly, a random sample for each related pair was removed.

#### Replication

**Simulations:** Each simulation setting was repeated for 20 times. Results were consistent across replicates, with the mean and distribution reported in the manuscript.

**Biobank analysis:** The target dataset was randomly and evenly divided into the validation and testing datasets for 100 times. Results were consistent across replicates, with the mean and standard deviation reported in the manuscript.

**Schizophrenia:** The analysis was performed on six independent testing cohorts. Results were consistent across six cohorts, with the full results reported in the manuscript.

#### Randomization

**Simulations:** Phenotypes and genotypes for individuals were randomly generated. Individuals were also randomly assigned into discovery, validation and testing datasets.

**Biobank analysis:** Individuals were randomly assigned into validation and testing datasets. Discovery GWAS summary statistics were directly obtained from peer-reviewed publications.

**Schizophrenia analysis:** We evaluated the predictive performance in every cohort using a leave-one-out scheme. The full results were reported and consistent with each other.

#### Blinding

Investigators were blinded to group assignments.

## Reporting for specific materials, systems and methods

We require information from authors about some types of materials, experimental systems and methods used in many studies. Here, indicate whether each material, system or method listed is relevant to your study. If you are not sure if a list item applies to your research, read the appropriate section before selecting a response.

### Materials & experimental systems

n/a	Involved in the study
<input checked="" type="checkbox"/>	<input type="checkbox"/> Antibodies
<input checked="" type="checkbox"/>	<input type="checkbox"/> Eukaryotic cell lines
<input checked="" type="checkbox"/>	<input type="checkbox"/> Palaeontology and archaeology
<input checked="" type="checkbox"/>	<input type="checkbox"/> Animals and other organisms
<input type="checkbox"/>	<input checked="" type="checkbox"/> Human research participants
<input checked="" type="checkbox"/>	<input type="checkbox"/> Clinical data
<input checked="" type="checkbox"/>	<input type="checkbox"/> Dual use research of concern

### Methods

n/a	Involved in the study
<input checked="" type="checkbox"/>	<input type="checkbox"/> ChIP-seq
<input checked="" type="checkbox"/>	<input type="checkbox"/> Flow cytometry
<input checked="" type="checkbox"/>	<input type="checkbox"/> MRI-based neuroimaging

## Human research participants

Policy information about [studies involving human research participants](#)

#### Population characteristics

UKBB is a population-based prospective study of approximately 500,000 voluntary participants, with ages ranging between 40 and 69 years, that were recruited between 2006 and 2010 across Great Britain.

BBJ is a registry of patients diagnosed with any of the 47 target common diseases. Patients were enrolled at 12 cooperative medical institutes all over Japan from June 2003 to March 2008. During the 5-year period, 200,000 participants were registered in the study. 53.1% of the subjects in BBJ were male and the average age at entry was 62.7 years for men and 61.5 years for women.

PAGE is a genetic epidemiology study with samples drawn from three existing major population-based cohorts. Genotyped

individuals were self-identified as Hispanic/Latino (n = 22,216), African American (n = 17,299), Asian (n = 4,680), Native Hawaiian (n = 3,940), Native American (n = 652) or Other (n = 1,052).

The Taiwan Biobank (TWB) is a prospective cohort study of the Taiwanese population. Participants were 30 to 70 years old at recruitment. We used 14,232 samples genotyped on the TWBv2 custom array, the same dataset used in the PRS analysis of our recent TWB quantitative trait GWAS study (Chen et al. MedRxiv 2021). Following the same sample-level and variant-level QC procedures used in the UKBB analysis, the final analytic sample included 10,149 unrelated individuals of EAS ancestry that had complete data across the 21 traits examined.

**Schizophrenia analysis:** Discovery GWAS of EUR and EAS ancestry were obtained from the Psychiatric Genomics Consortium as reported and referenced. EAS target cohorts: except for TMIM1, all samples were included in a previous publication (Lam et al. Nature Genetics 2019), where detailed description of each cohort can be found. TMIM1 cohort has 3,376 cases and 3,501 controls of Japanese ancestry post QC.

#### Recruitment

Except for TMIM1 (described below), all schizophrenia cohorts used in this study and their recruitment protocols have been reported in previous publications. We have cited these publications where relevant.

Subjects in TMIM1 were recruited from multiple university hospitals and local hospitals in Japan. Patients were diagnosed according to the Diagnostic and Statistical Manual of Mental Disorders, 4th Edition (DSM-IV) with consensus from at least two experienced psychiatrists. All patients agreed to participate in the study and provided written informed consent. There could be potential bias towards patients who are more willing to consent for this study (e.g., patients in remission or in good cognition state). This bias reduces the statistical power to find genetic factors underlying severe and/or treatment-resistant schizophrenia subtypes. This bias, however, does not affect our conclusion as it applies to all European and East Asian subjects and does not change the relative predictive performance of different polygenic prediction methods examined in this study.

#### Ethics oversight

Collection of the UKBB data was approved by the UKBB's Research Ethics Committee. UKBB individual-level data used in the present work were obtained under application #32568. BBJ and PAGE: only publicly available GWAS summary statistics, without individual-level information, were used in this study. Collection of the TWB data was approved by the Ethics and Governance Council (EGC) of TWB and the Department of Health and Welfare, Taiwan (Wei-Shu-I-Tzu NO.1010267471). TWB obtained informed consent from all participants for research use of the collected data. The access to and the use of TWB data in the present work was approved by the EGC of TWB (approval number: TWBR10907-05) and the Institutional Review Board of National Health Research Institutes, Taiwan (approval number: EC1090402-E). Schizophrenia GWAS summary statistics of EUR and EAS ancestries are available via the Psychiatric Genomics Consortium, and do not contain any individual-level information. The following institutions provided ethics oversight for schizophrenia East Asian samples used in this work: Samsung Medical Center; Bio-X Institutes of Shanghai Jiao Tong University; Fujita Health University; Tokyo Metropolitan Institute of Medical Science; University Medical Center Utrecht; The University of Western Australia; The University of Indonesia; RIKEN Center for Integrative Medical Sciences; Nagoya University; Osaka University; Niigata University; Chonnam National University Hospital, and Mass General Brigham (Protocols 2014P001342 and 2011P002207). Informed consent and permission to share the data were obtained from all subjects, in compliance with the guidelines specified by the recruiting center's institutional review board.

Note that full information on the approval of the study protocol must also be provided in the manuscript.